دیاگرام های فازی

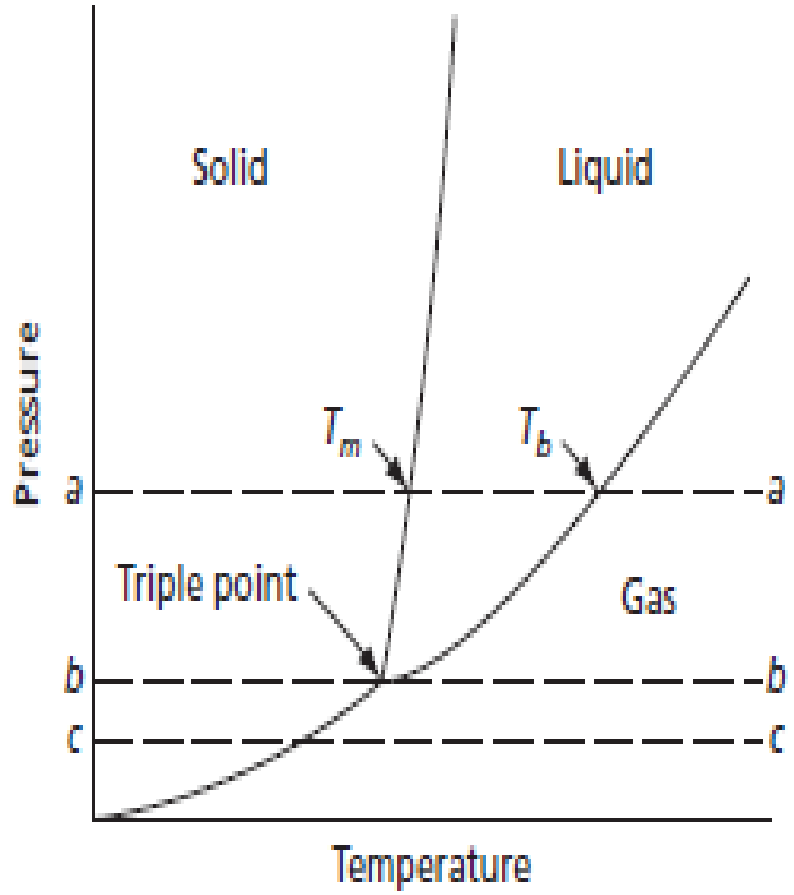

FIG. 14.2 Same as Fig. 14.1, but showing the isobars considered in Fig. 14.3

مقایسه منحنی های سرد شدن یک فلز خالص ویک الیاژ

The Cooling Curve

- Cooling curve indicates the gradual change in temperature with time during cooling of alloy

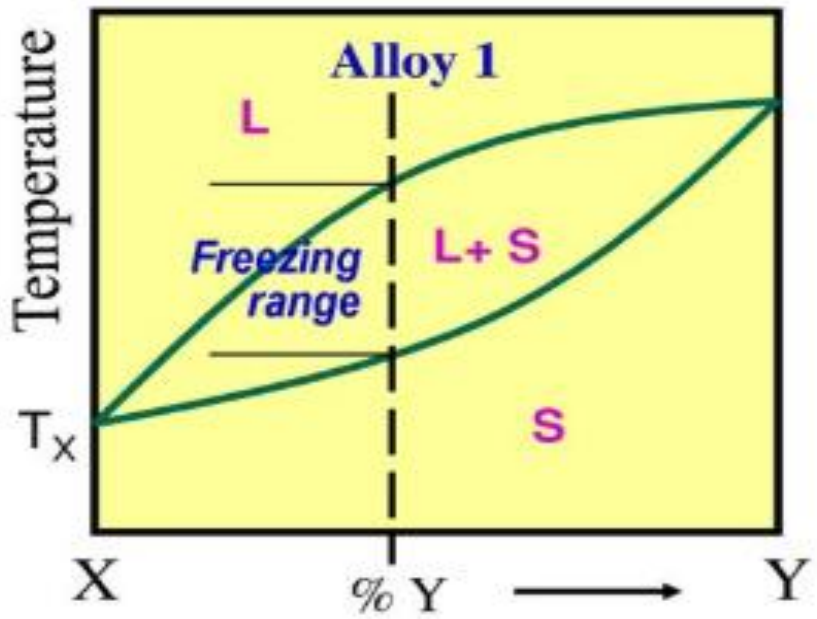

سرعت سرد شدن- زمان انجماد

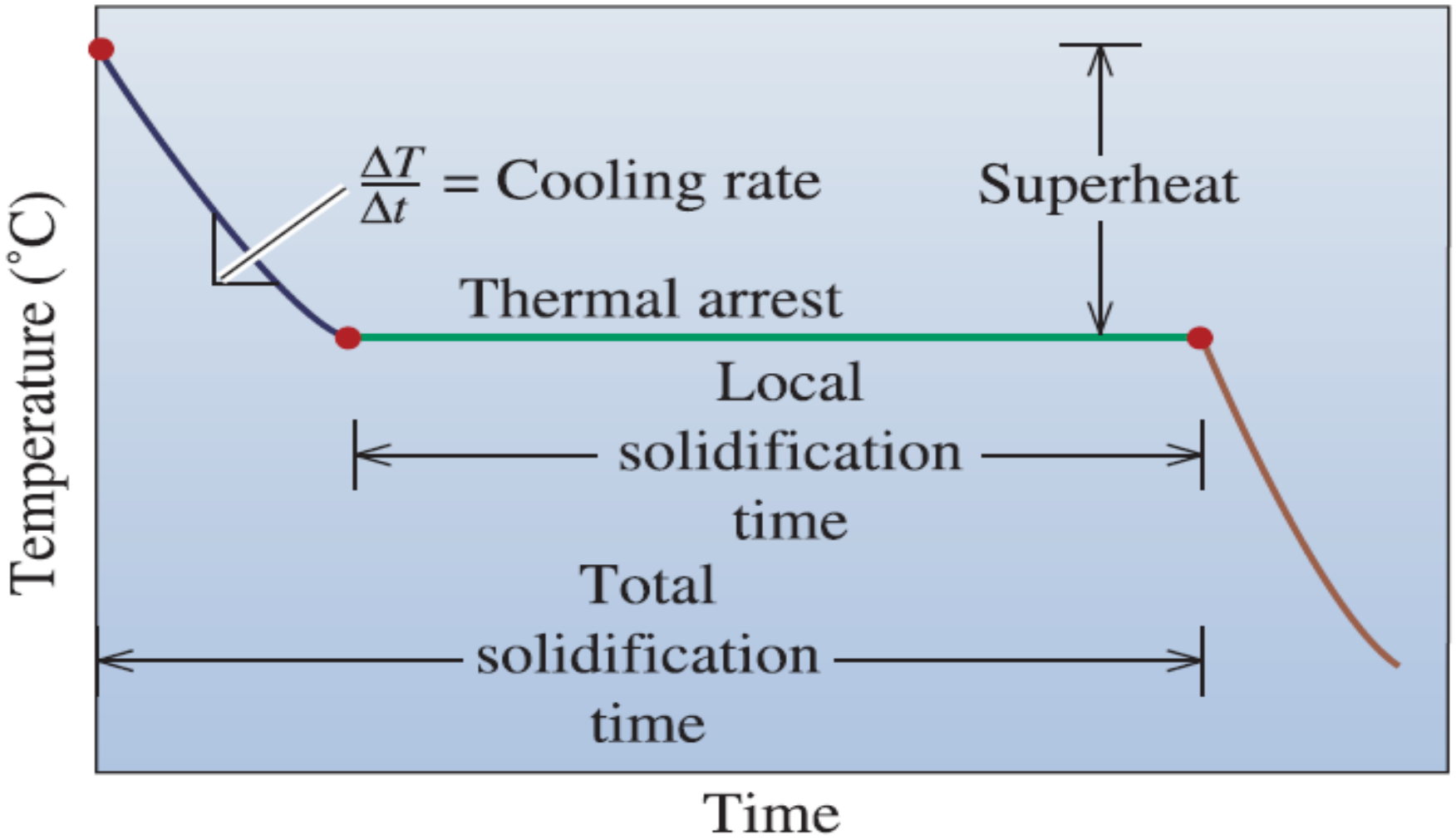

انجماد فلز خالص مس

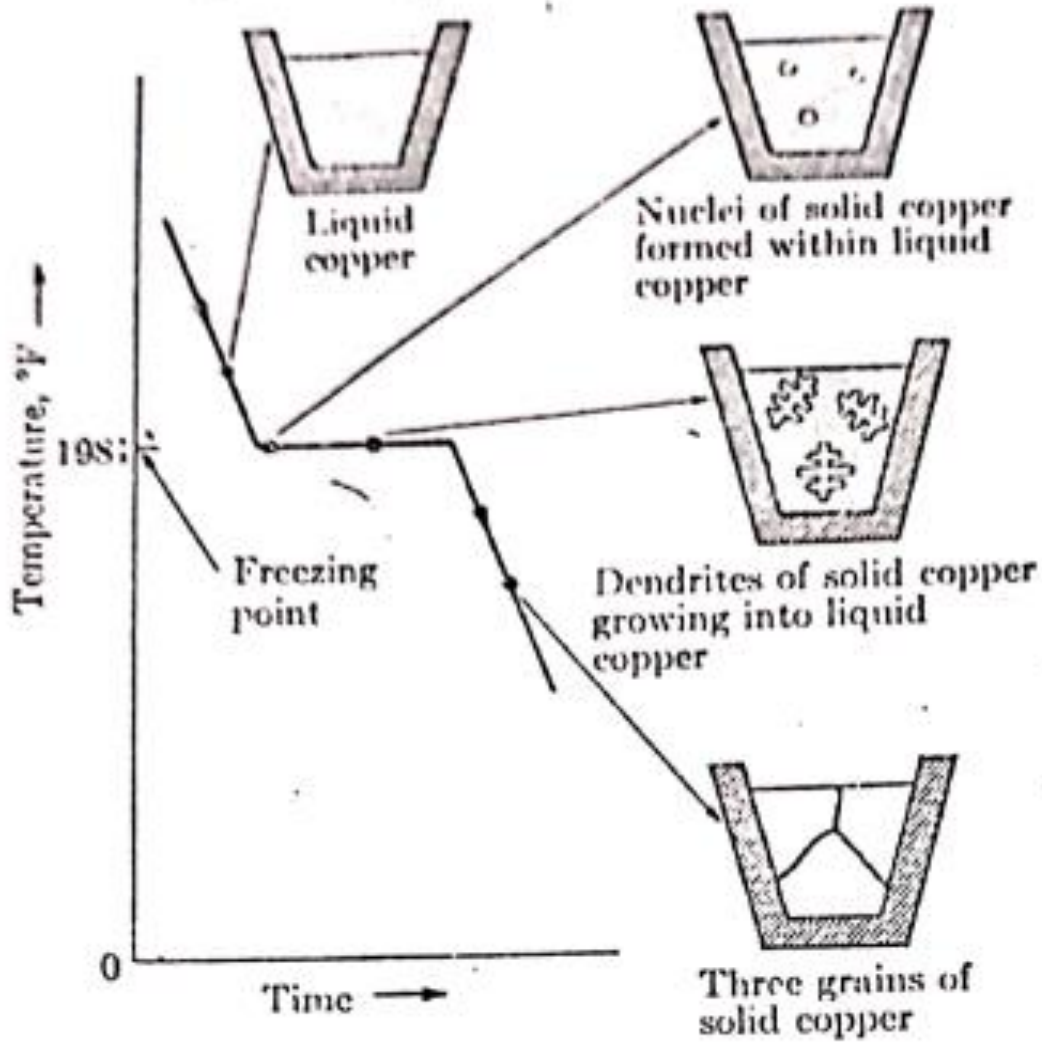

FIG. 6–2. Time-temperature curve for the solidification of a small crucible of liquid copper.

انجماد فلز خالص انتیموان

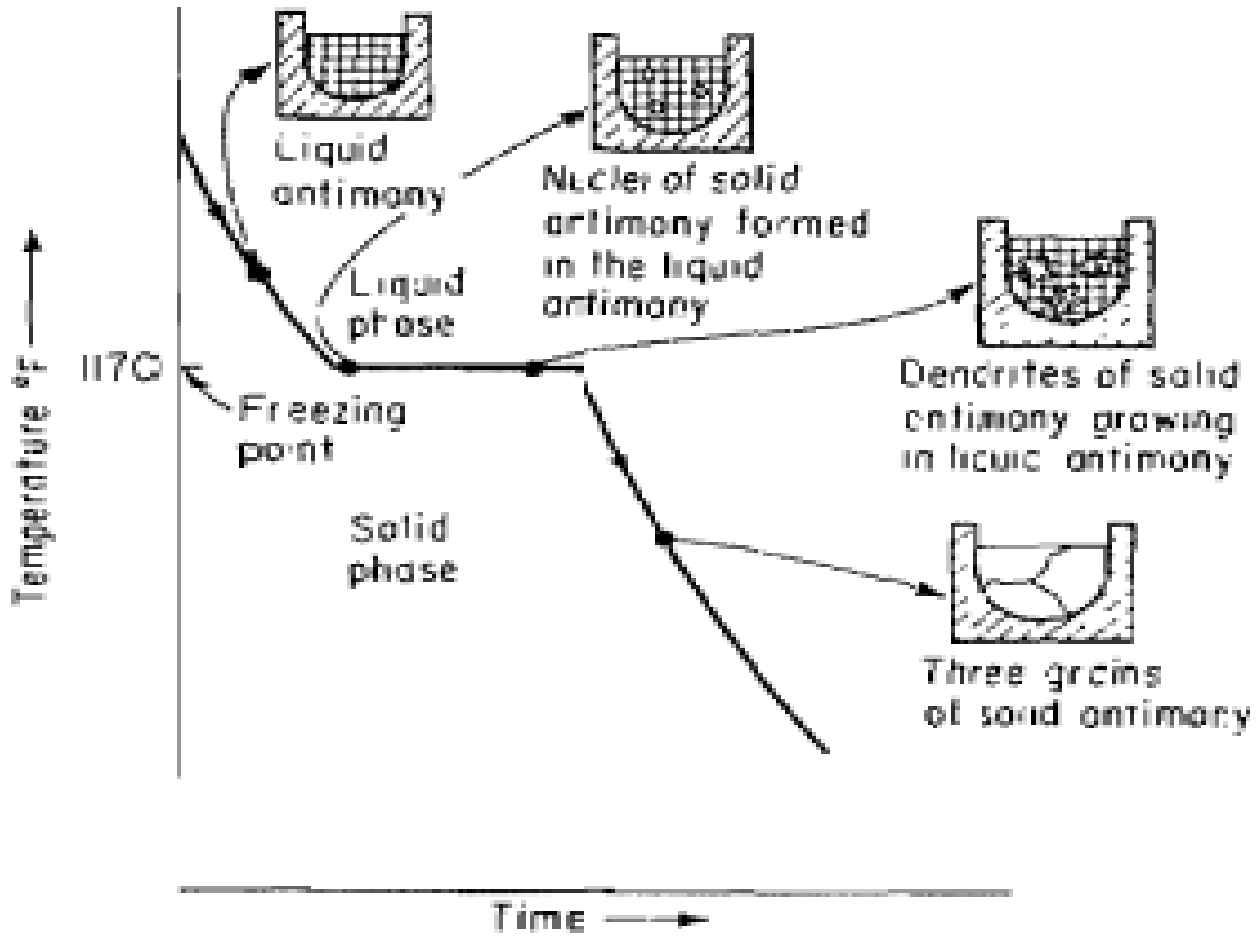

Fig. 5-1 Time-temperature cooling curve for the solidification of a small crucible of liquid antimony.

منحنی سرد شدن- دیاگرام محلول جامد

Cooling Curves

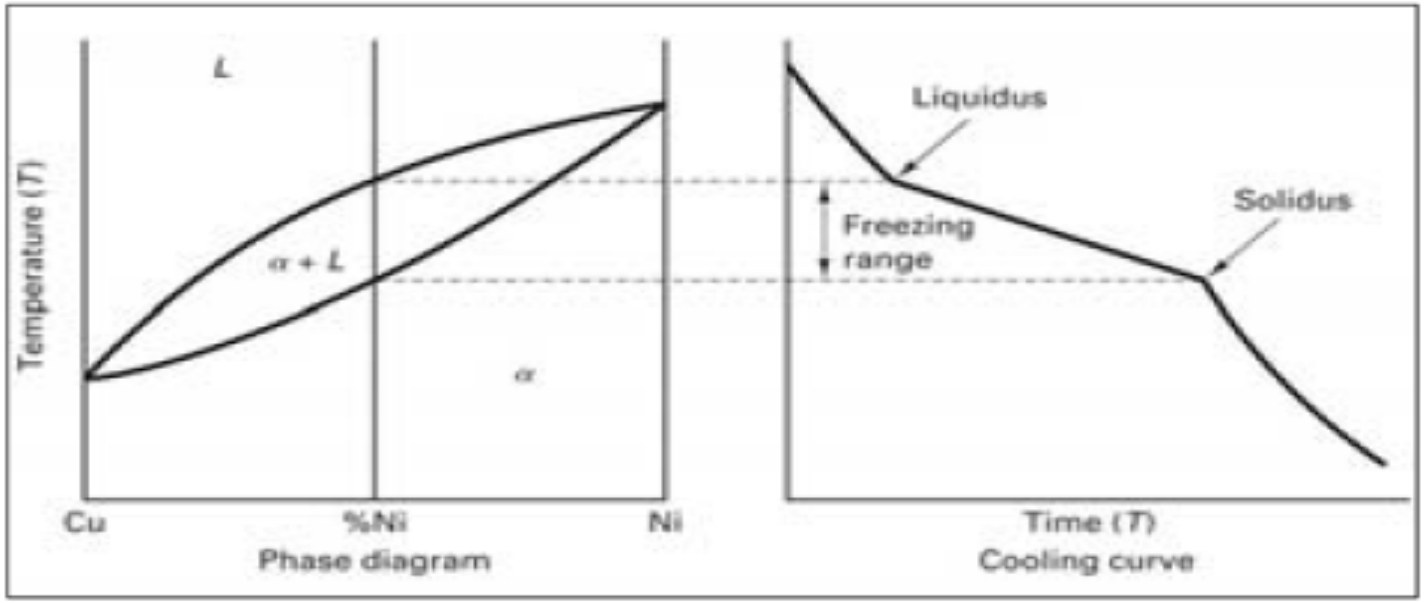

Figure 11-4 Phase diagram and companion cooling curve for an alloy with a freezing range. The slope changes indicate the onset and termination of solidification.

منحنی سرد شدن الیاژ مس -نیکل

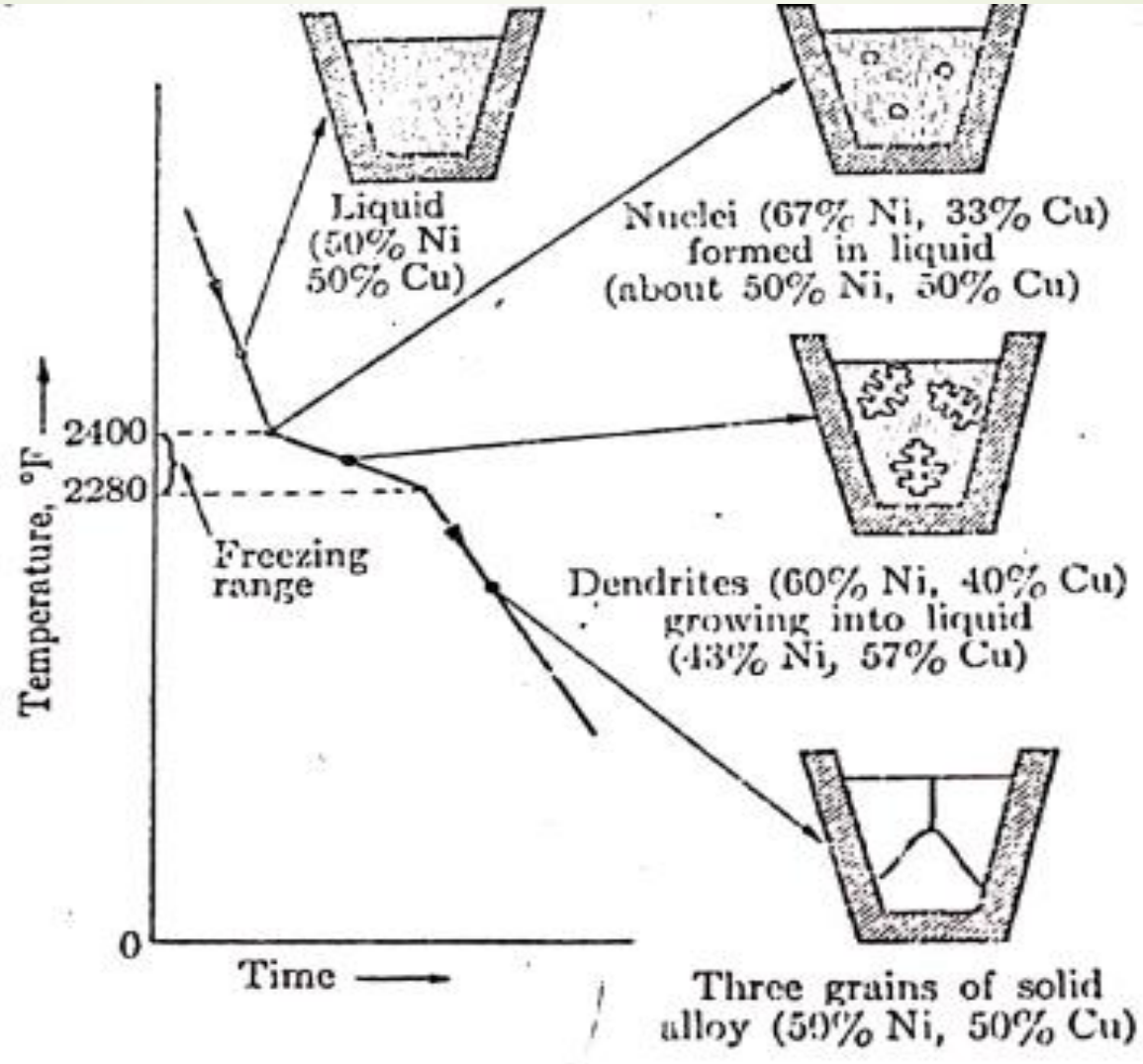

FIG. 6–3. Time-temperature curve for the solidification of a small crucible of 50% copper, 50% nickel alloy.

انجماد الياژانتيموان بيسموت

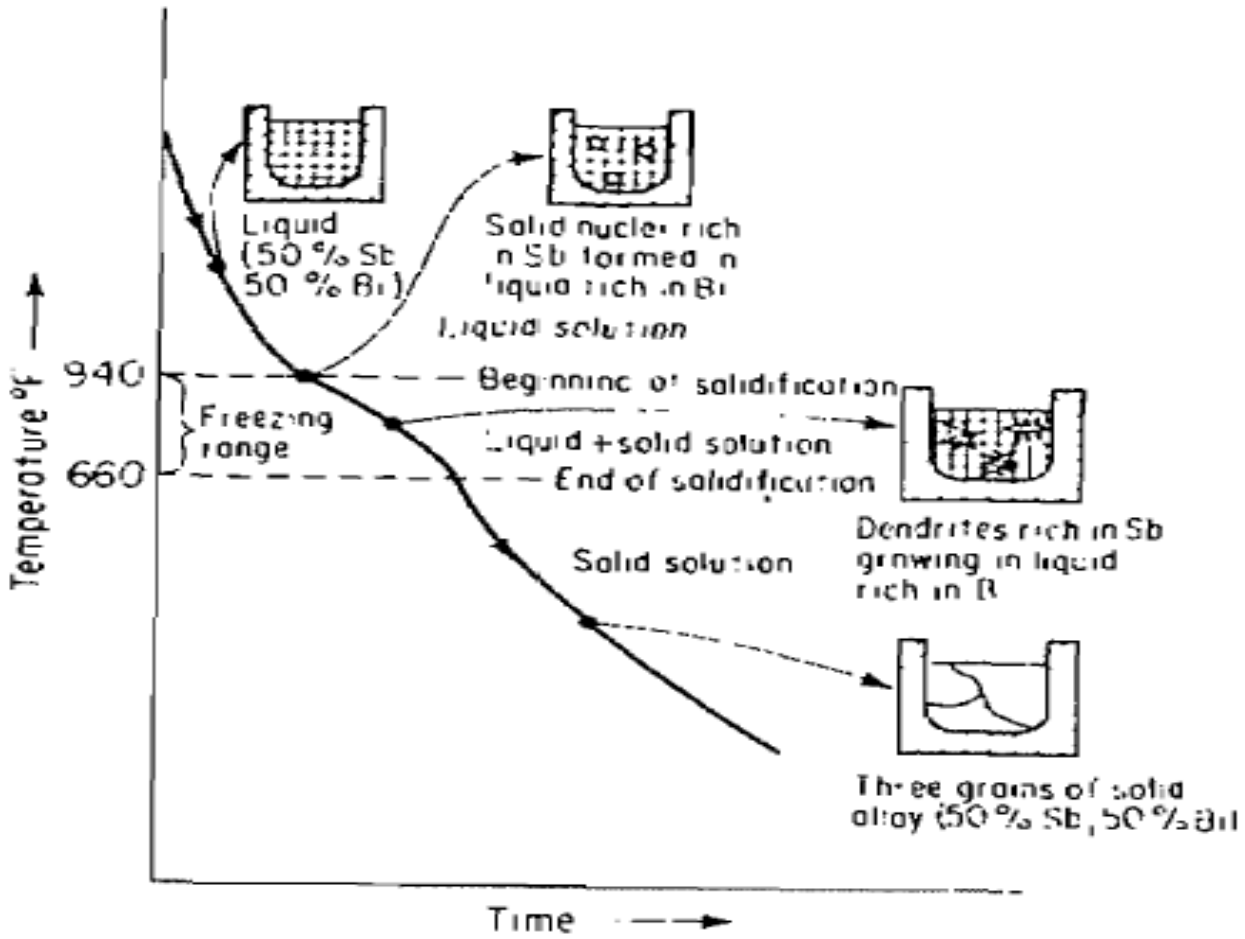

Fig. 5-2 Time-temperature cooling curve for the solidification of a small crucible of 50 percent antimony, 50 percent bismuth alloy.

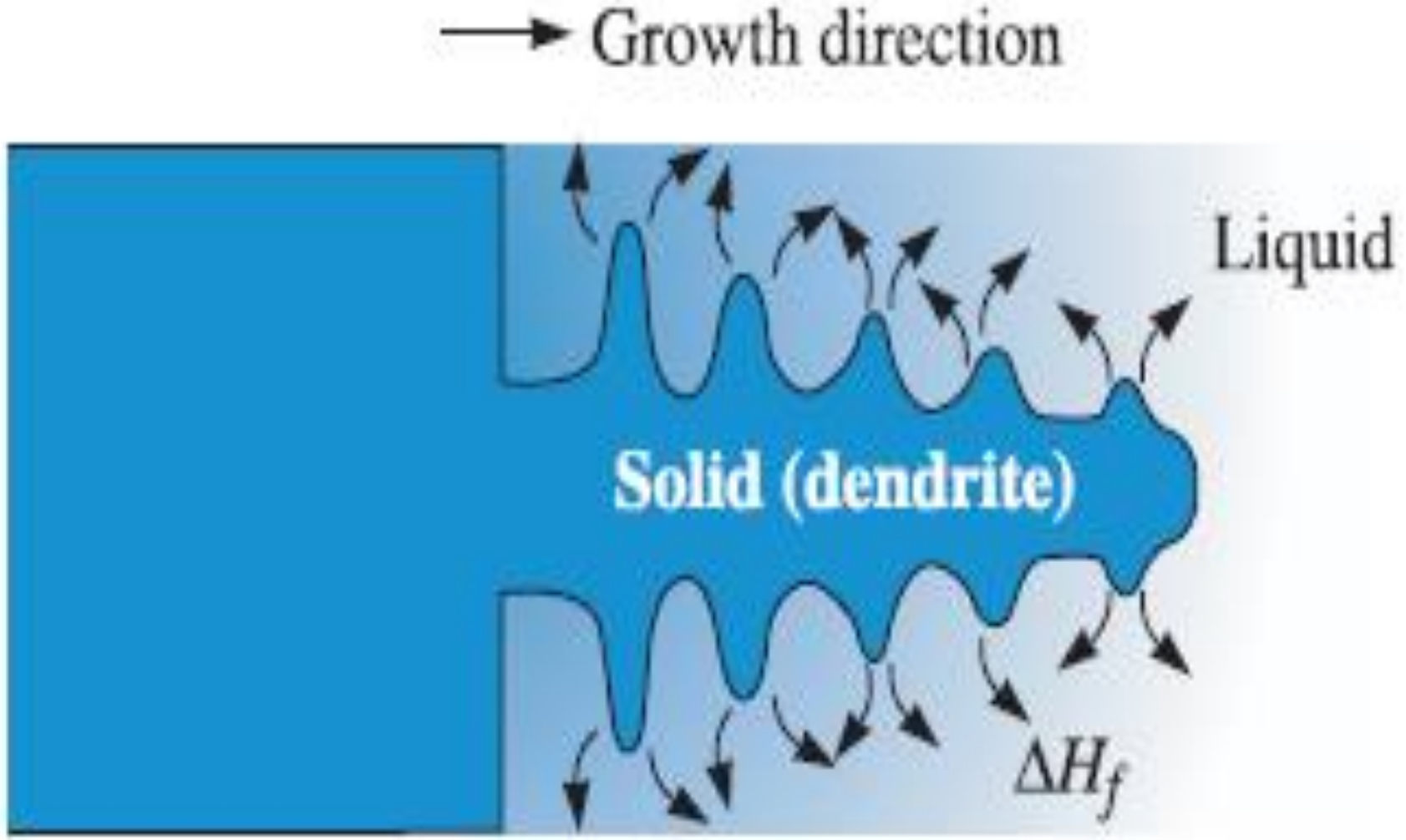
Growth direction
Liquid
Solid (dendrite)
ΔH_f

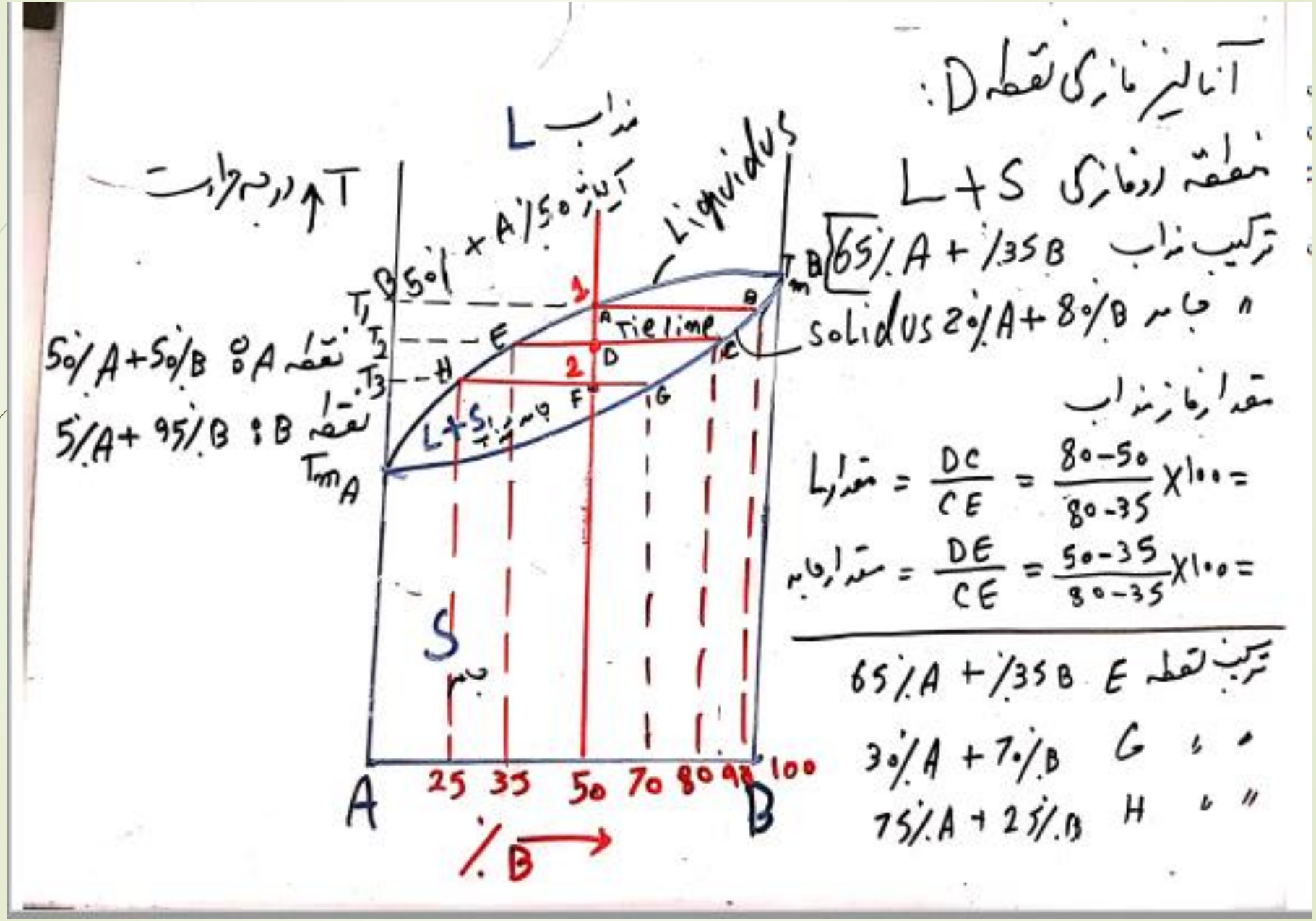
آنالیز فازی نقطه D:
منطقه دوفازی L+S
ترکیب مذاب 65٪A + ٪35B
" جامد 20٪A + 80٪B
مقدار فاز مذاب
ترکیب نقطه E 65٪A + ٪35B
" " G 30٪A + 70٪B
" " H 75٪A + 25٪B
L مذاب
T افزایش درجه حرارت
Liquidus
solidus
Tie line
50٪ A + ٪50 B آلیاژ
50٪A + 50٪B نقطه 1
5٪A + 95٪B نقطه 2
L+S
S جامد
A
B
25 35 50 70 80 95 100
٪B

دیاگرام محلول جامد

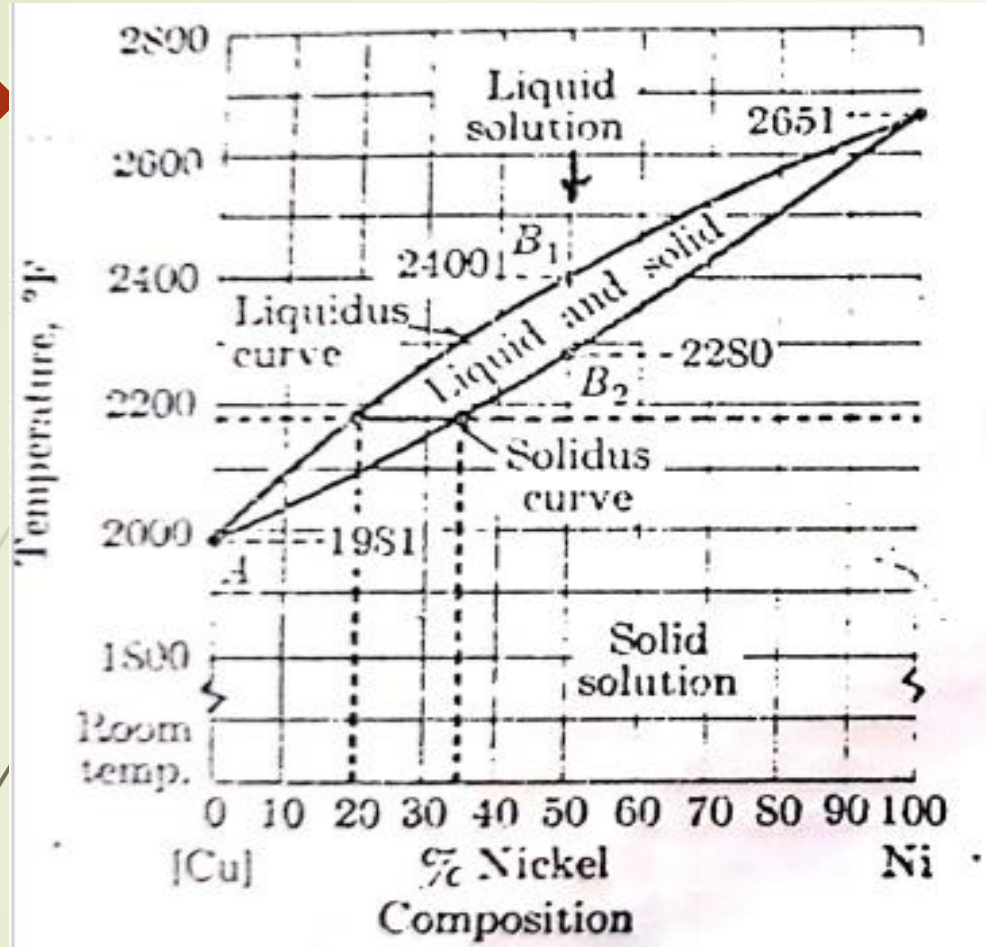

FIG. 6–4. The copper-nickel equilibrium diagram. Points A, B_1, and B_2 show how the diagram is constructed from time-temperature curve data.

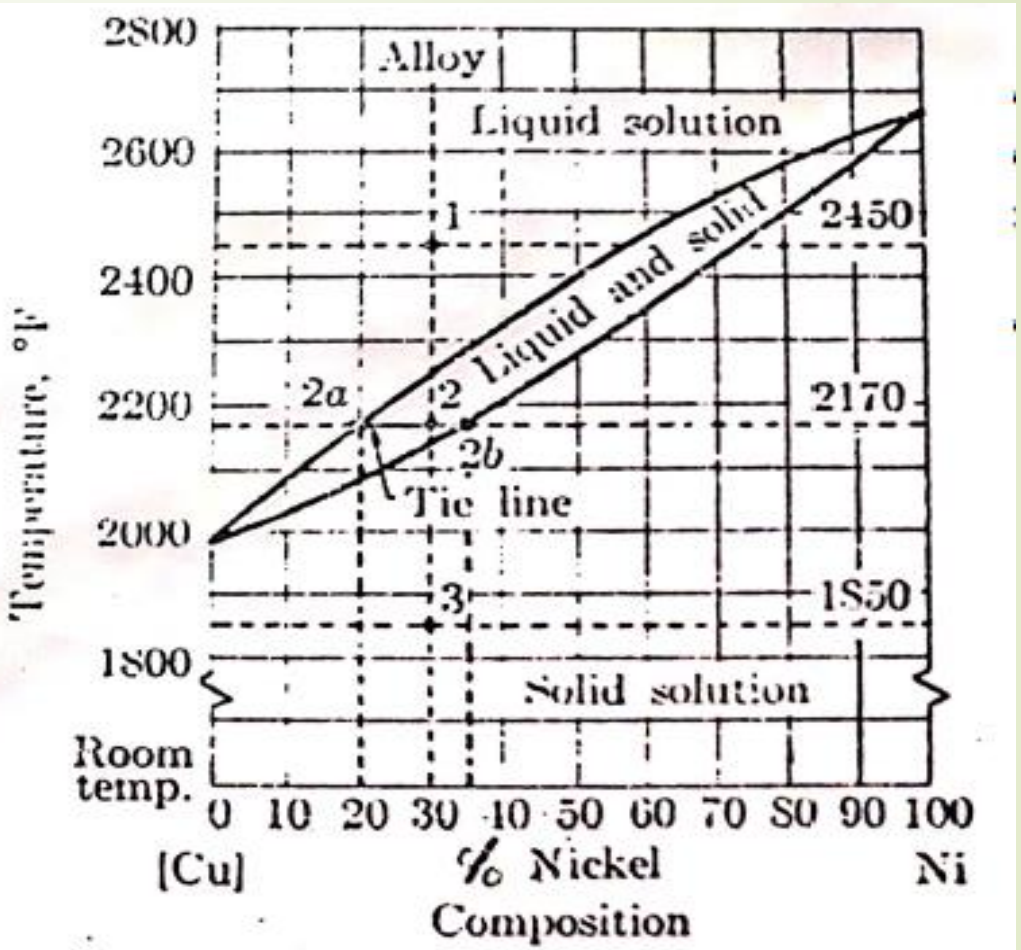

FIG. 6–5. The equilibrium conditions of a 30% nickel alloy at three different temperatures.

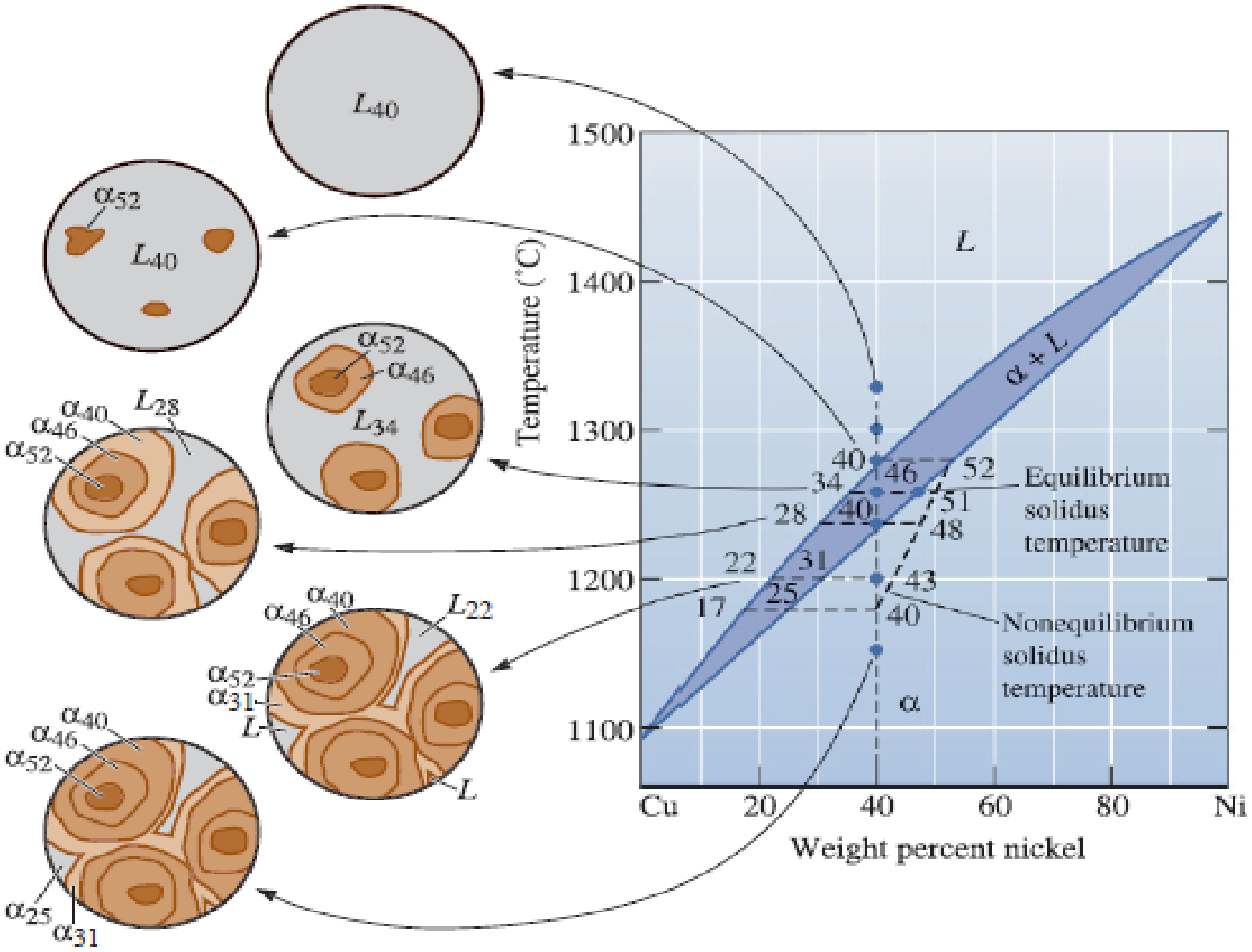

Figure 10-17 The change in structure of a Cu-40% Ni alloy during nonequilibrium solidification. Insufficient time for diffusion in the solid produces a segregated structure. Notice the nonequilibrium solidus curve.

Example 10-11 *Nonequilibrium Solidification of Cu-Ni Alloys*

Calculate the composition and amount of each phase in a Cu-40% Ni alloy that is present under the nonequilibrium conditions shown in Figure 10-17 at 1300°C, 1280°C, 1260°C, 1240°C, 1200°C, and 1150°C. Compare with the equilibrium compositions and amounts of each phase.

SOLUTION

We use the tie line to the equilibrium solidus temperature to curve to calculate compositions and percentages of phases as per the lever rule. Similarly, the nonequilibrium solidus temperature curve is used to calculate percentages and concentrations of different phases formed under nonequilibrium conditions.

Temperature	Equilibrium	Nonequilibrium
1300°C	L: 40% Ni 100% L	L: 40% Ni 100% L
1280°C	L: 40% Ni 100% L	L: 40% Ni 100% L
1260°C	L: 34% Ni $\frac{46-40}{46-34} = 50\%\ L$	L: 34% Ni $\frac{51-40}{51-34} = 65\%\ L$
	α: 46% Ni $\frac{40-34}{46-34} = 50\%\ \alpha$	α: 51% Ni $\frac{40-34}{51-34} = 35\%\ \alpha$
1240°C	L: 28% Ni ~ 0% L	L: 28% Ni $\frac{48-40}{48-28} = 40\%\ L$
	α: 40% Ni 100% α	α: 48% Ni $\frac{40-28}{48-28} = 60\%\ \alpha$
1200°C	α: 40% Ni 100% α	L: 22% Ni $\frac{43-40}{43-22} = 14\%\ L$
		α: 43% Ni $\frac{40-22}{43-22} = 86\%\ \alpha$
1150°C	α: 40% Ni 100% α	α: 40% Ni 100% α

دیاگرام محلول جامد(درصدجامد ومذاب)

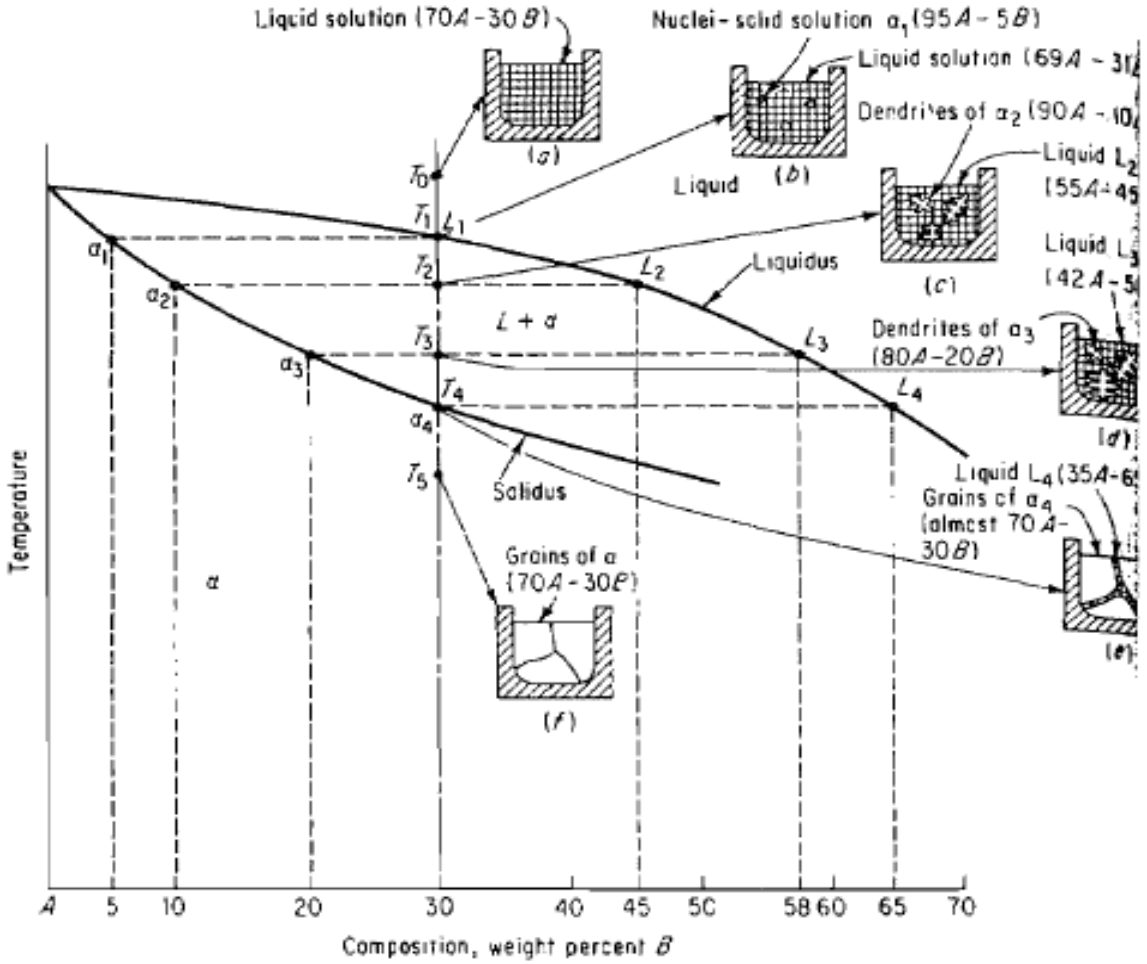

Fig. 6-5 The slow cooling of a 70A-30B alloy, showing the microstructure at various points during solidification.

دیاگرام یوتکتیک

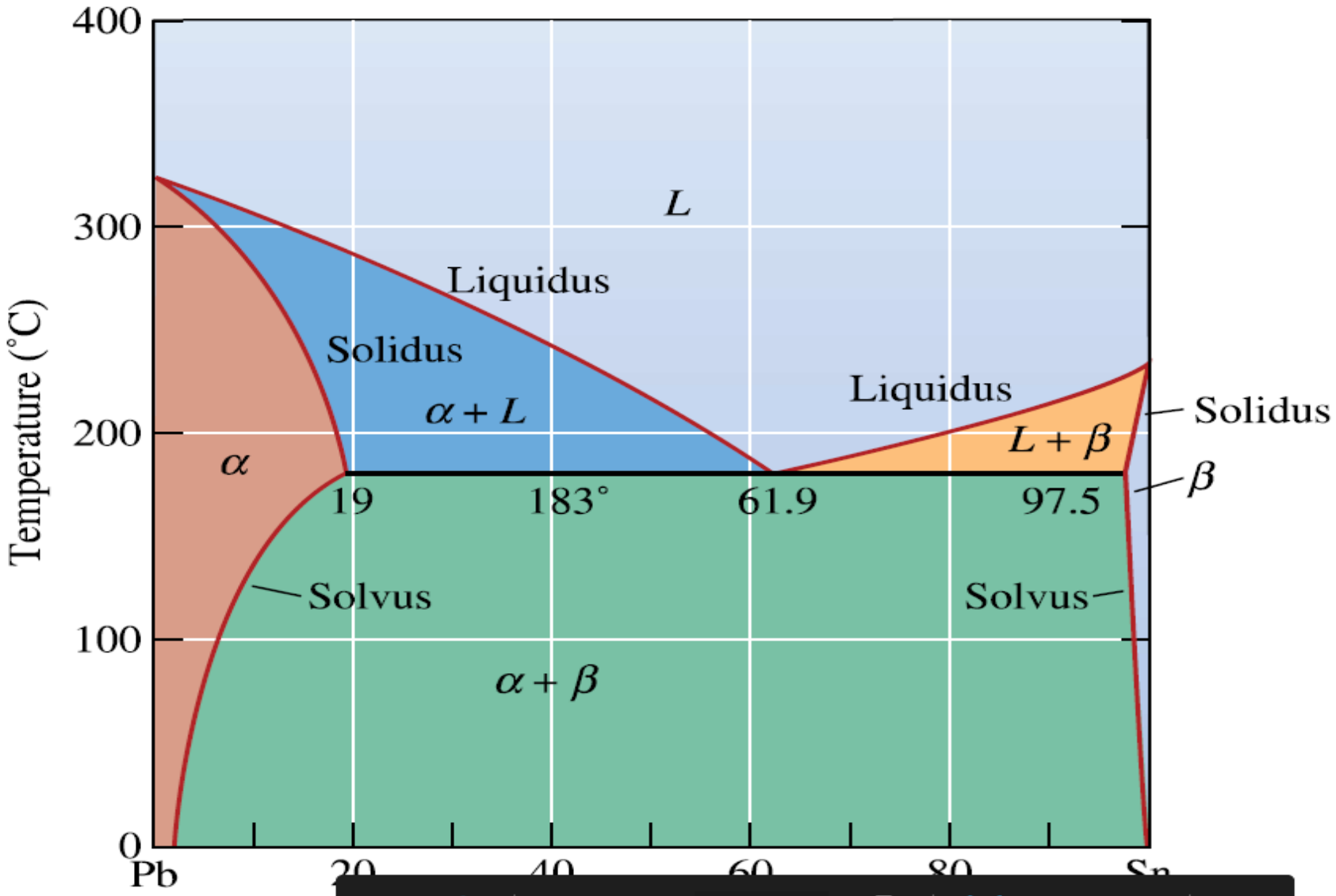

سه الیاژ با ترکیب متفاوت

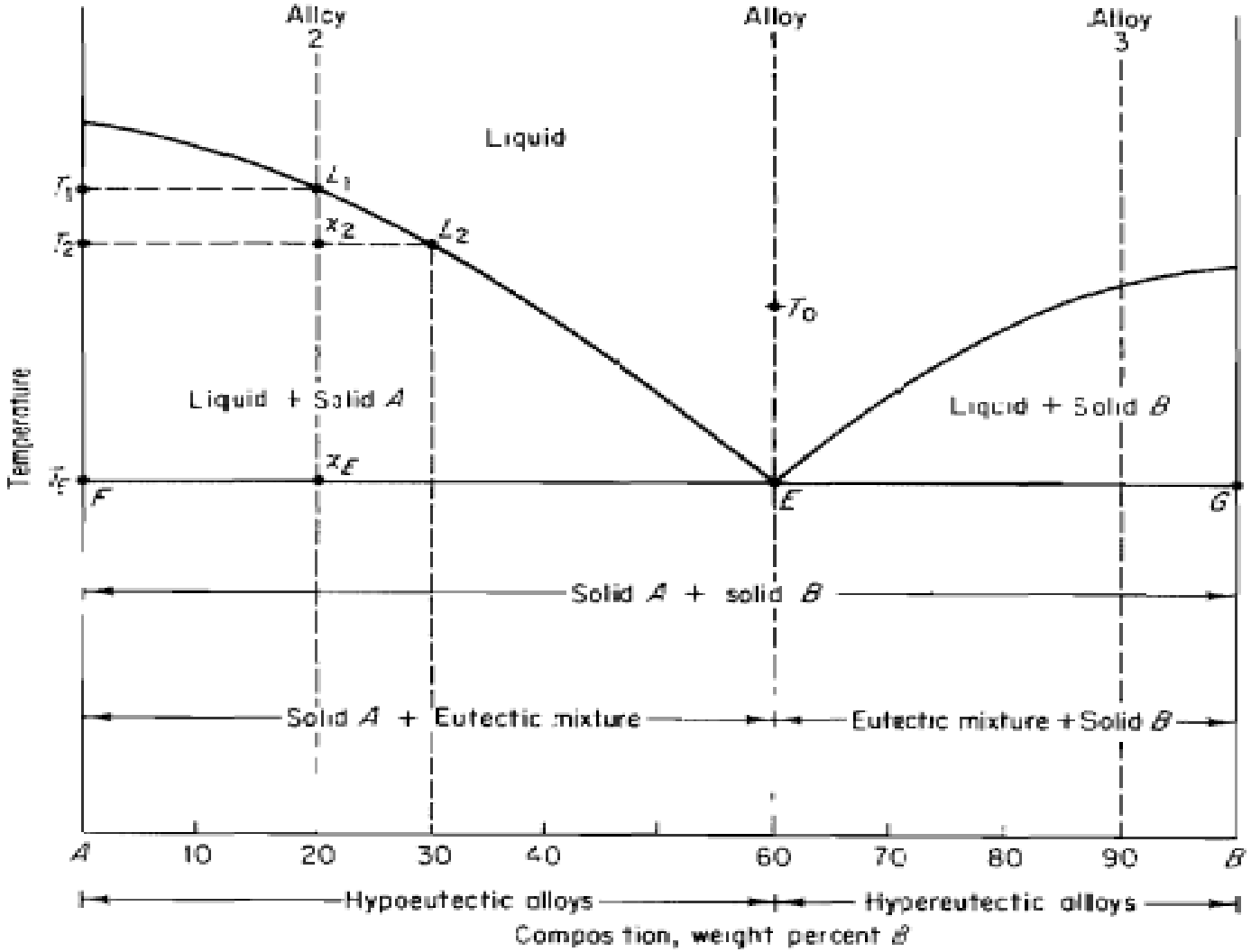

Fig. 6-17 Eutectic-type phase diagram.

دیاگرام یوتکتیک محلول جامد تک فاز

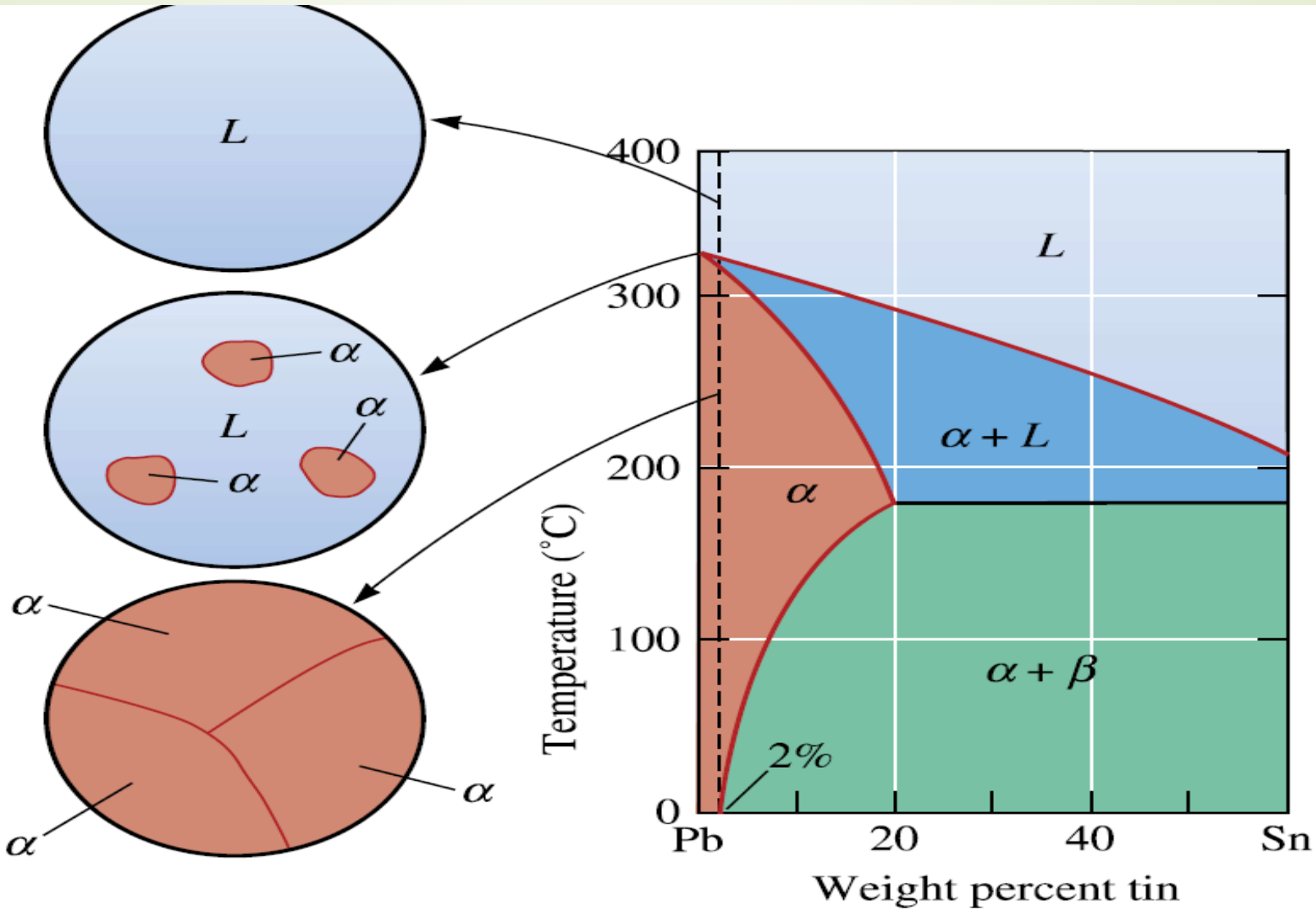

Figure 11-7 Solidification and microstructure of a Pb-2% Sn alloy. The alloy is a single-phase solid solution.

الیاژ یوتکتیک

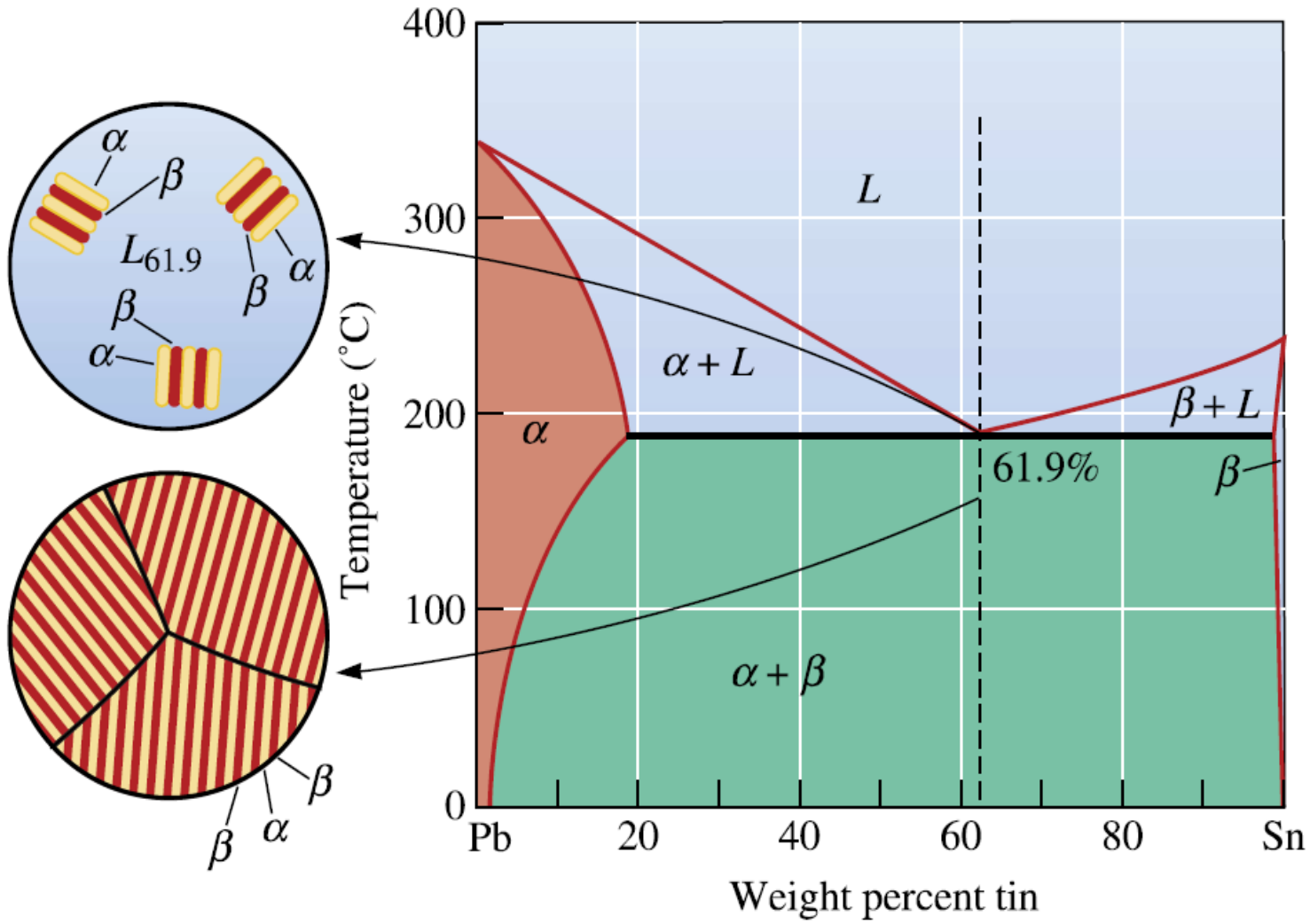

Figure 11-9 Solidification and microstructure of the eutectic alloy Pb-61.9% Sn.

ساختمان یوتکتیک

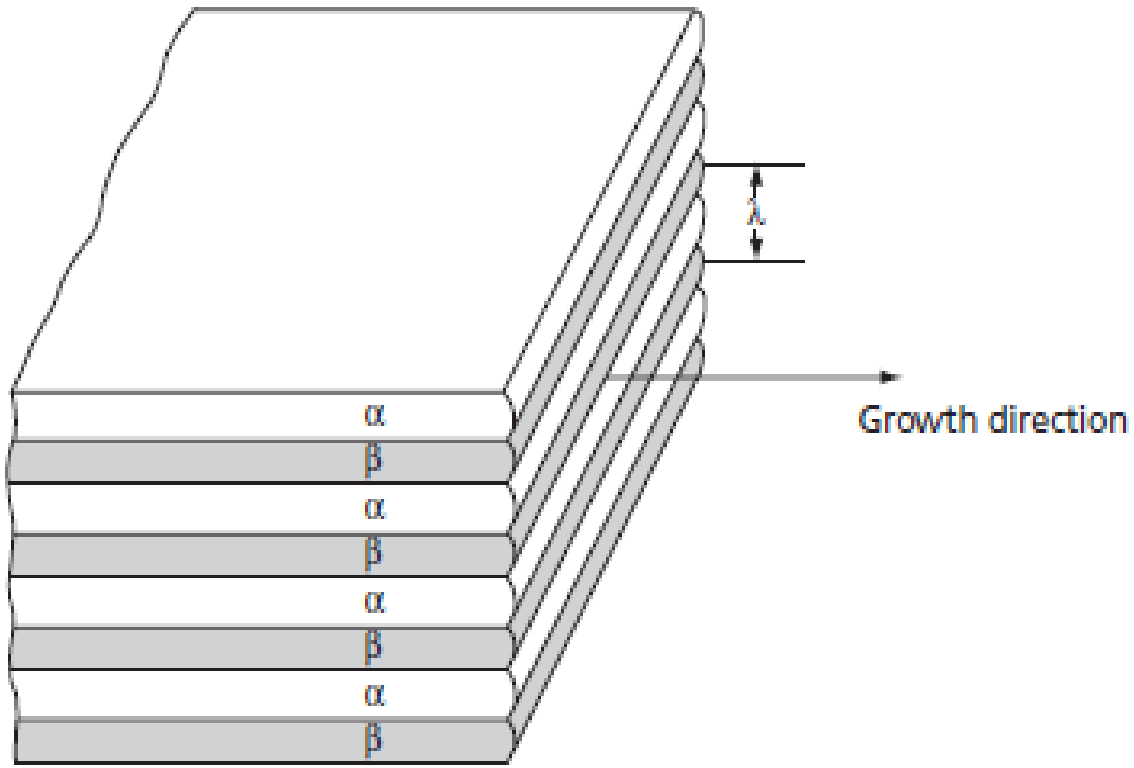

FIG. 14.43 Simple plate-like lamellar eutectic with an interarm spacing λ

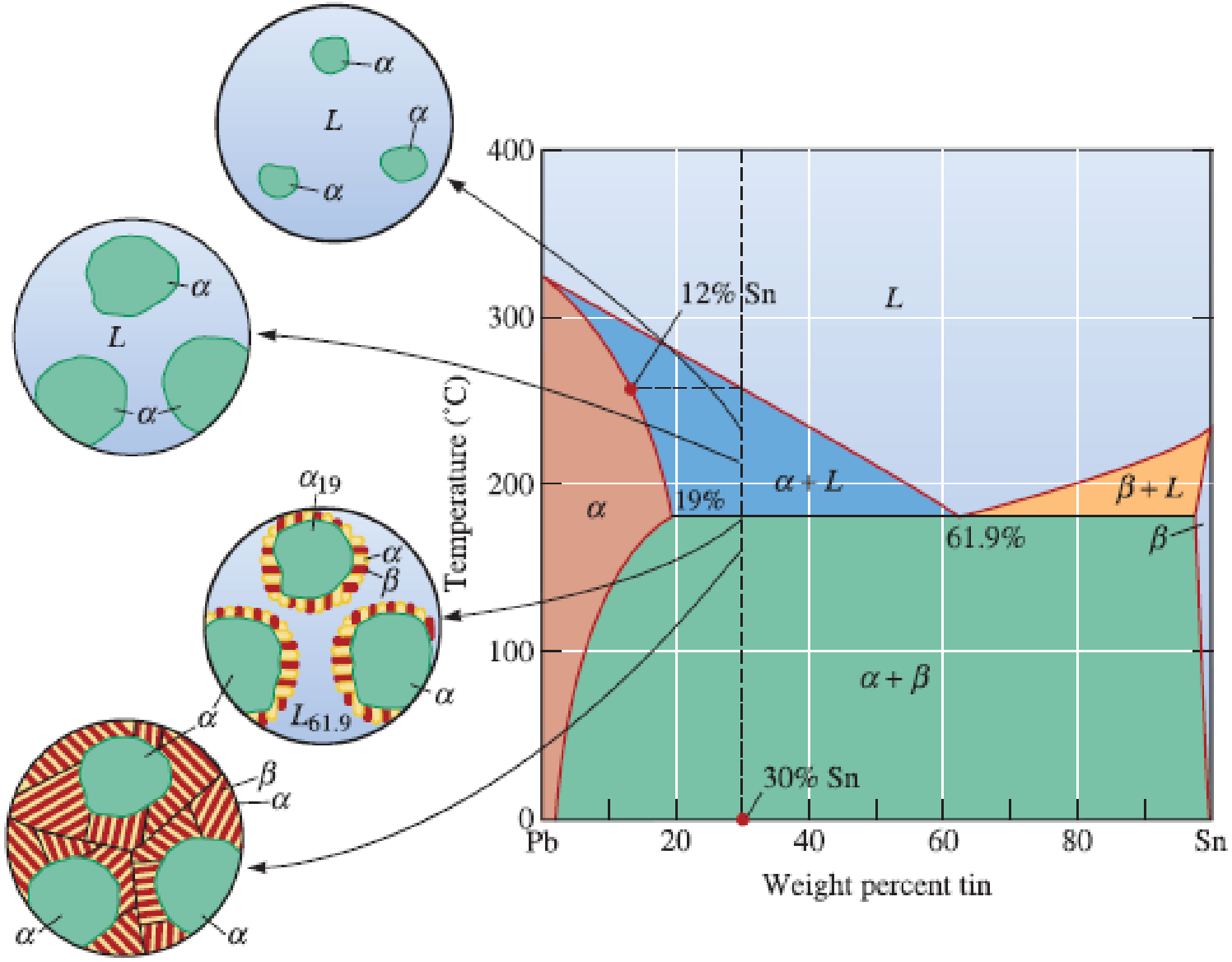

Figure 11-13 The solidification and microstructure of a hypoeutectic alloy (Pb-30% Sn).

Example 11-4 *Determination of Phases and Amounts in a Pb-30% Sn Hypoeutectic Alloy*

For a Pb-30% Sn alloy, determine the phases present, their amounts, and their compositions at 300°C, 200°C, 184°C, 182°C, and 0°C.

SOLUTION

Temperature (°C)	Phases	Compositions	Amounts
300	L	L: 30% Sn	$L = 100\%$
200	$\alpha + L$	L: 55% Sn	$L = \frac{30 - 18}{55 - 18} \times 100 = 32\%$
		α: 18% Sn	$\alpha = \frac{55 - 30}{55 - 18} \times 100 = 68\%$
184	$\alpha + L$	L: 61.9% Sn	$L = \frac{30 - 19}{61.9 - 19} \times 100 = 26\%$
		α: 19% Sn	$\alpha = \frac{61.9 - 30}{61.9 - 19} \times 100 = 74\%$
182	$\alpha + \beta$	α: 19% Sn	$\alpha = \frac{97.5 - 30}{97.5 - 19} \times 100 = 86\%$
		β: 97.5% Sn	$\beta = \frac{30 - 19}{97.5 - 19} \times 100 = 14\%$
0	$\alpha + \beta$	α: 2% Sn	$\alpha = \frac{100 - 30}{100 - 2} \times 100 = 71\%$
		β: 100% Sn	$\beta = \frac{30 - 2}{100 - 2} \times 100 = 29\%$

60A- 40Bدیاگرام یوتکتیک الیاژ درصد فازها

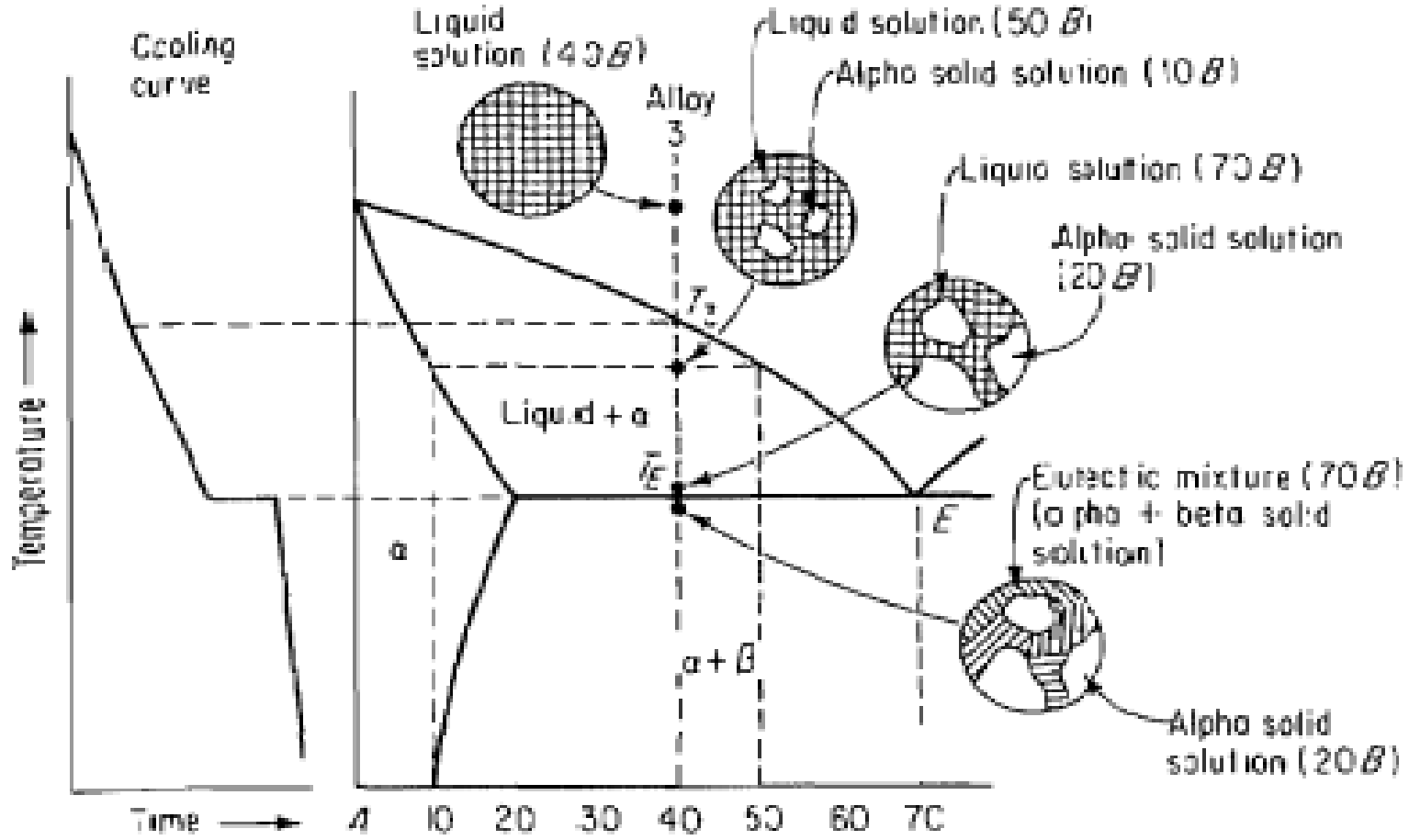

Fig. 6·27 The cooling curve and microstructure at various temperatures during solidification of a 60A-40B alloy.

دیاگرام یوتکتیک الیاژ درصد فازها برای سه الیاژ ۱و۲و۳

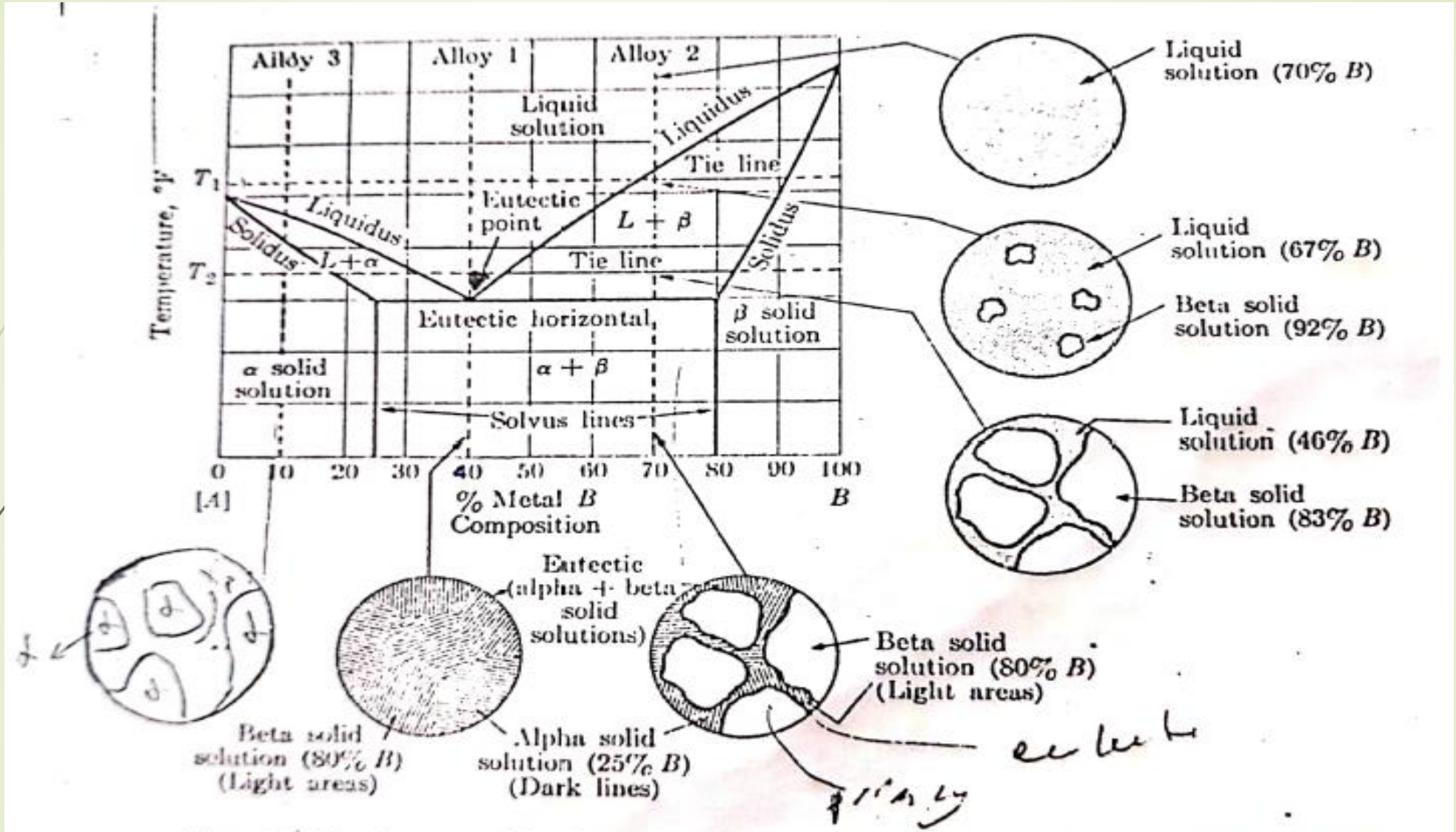

FIG. 6-12. A generalized eutectic equilibrium diagram involving the hypothetical metals A and B. The solidification processes of alloy 1 (eutectic composition) and of alloy 2 are indicated.

واکنشهای دیاگرامهای فازی

TABLE 6·4 Equilibrium-diagram Reactions

NAME OF REACTION	GENERAL EQUATION	APPEARANCE ON DIAGRAM
Monotectic	$L_1 \underset{\text{heating}}{\overset{\text{cooling}}{\rightleftharpoons}} L_2 + \text{solid}$	L_1 / $L_2 + \text{solid}$
Eutectic	$\text{Liquid} \underset{\text{heating}}{\overset{\text{cooling}}{\rightleftharpoons}} \text{solid}_1 + \text{solid}_2$	L / $\text{Solid}_1 + \text{solid}_2$
Eutectoid	$\text{Solid}_1 \underset{\text{heating}}{\overset{\text{cooling}}{\rightleftharpoons}} \text{solid}_2 + \text{solid}_3$	Solid_1 / $\text{Solid}_2 + \text{solid}_3$
Peritectic	$\text{Liquid} + \text{solid}_1 \underset{\text{heating}}{\overset{\text{cooling}}{\rightleftharpoons}} \text{new solid}_2$	$\text{Liquid} + \text{solid}_1$ / New solid_2
Peritectoid	$\text{Solid}_1 + \text{solid}_2 \underset{\text{heating}}{\overset{\text{cooling}}{\rightleftharpoons}} \text{new solid}_3$	$\text{Solid}_1 + \text{solid}_2$ / New solid_3

دیاگرام پری تکتیک

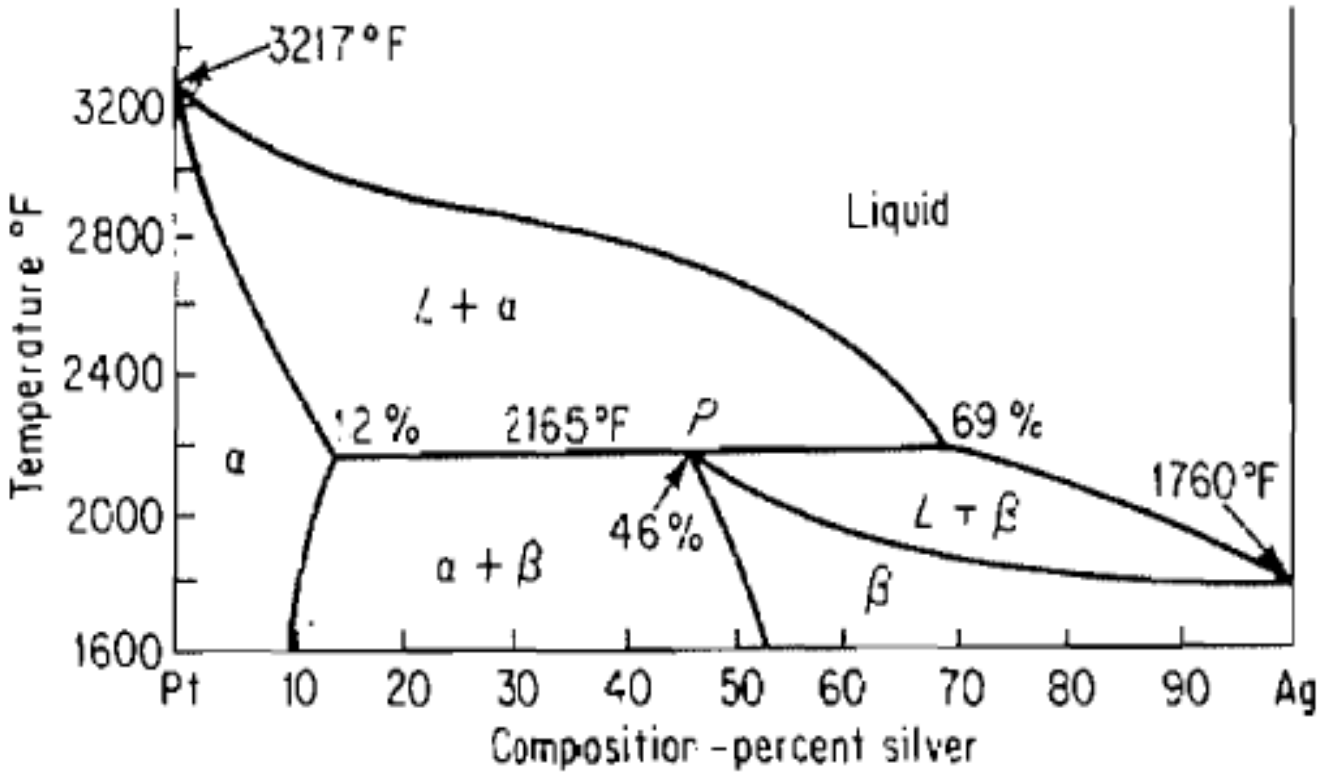

Fig. 6-39 Silver-platinum alloy system showing the formation of a terminal solid solution by a peritectic reaction.

دیاگرام پری تکتیک نقره پلاتین فاز ها ودرصد فازها

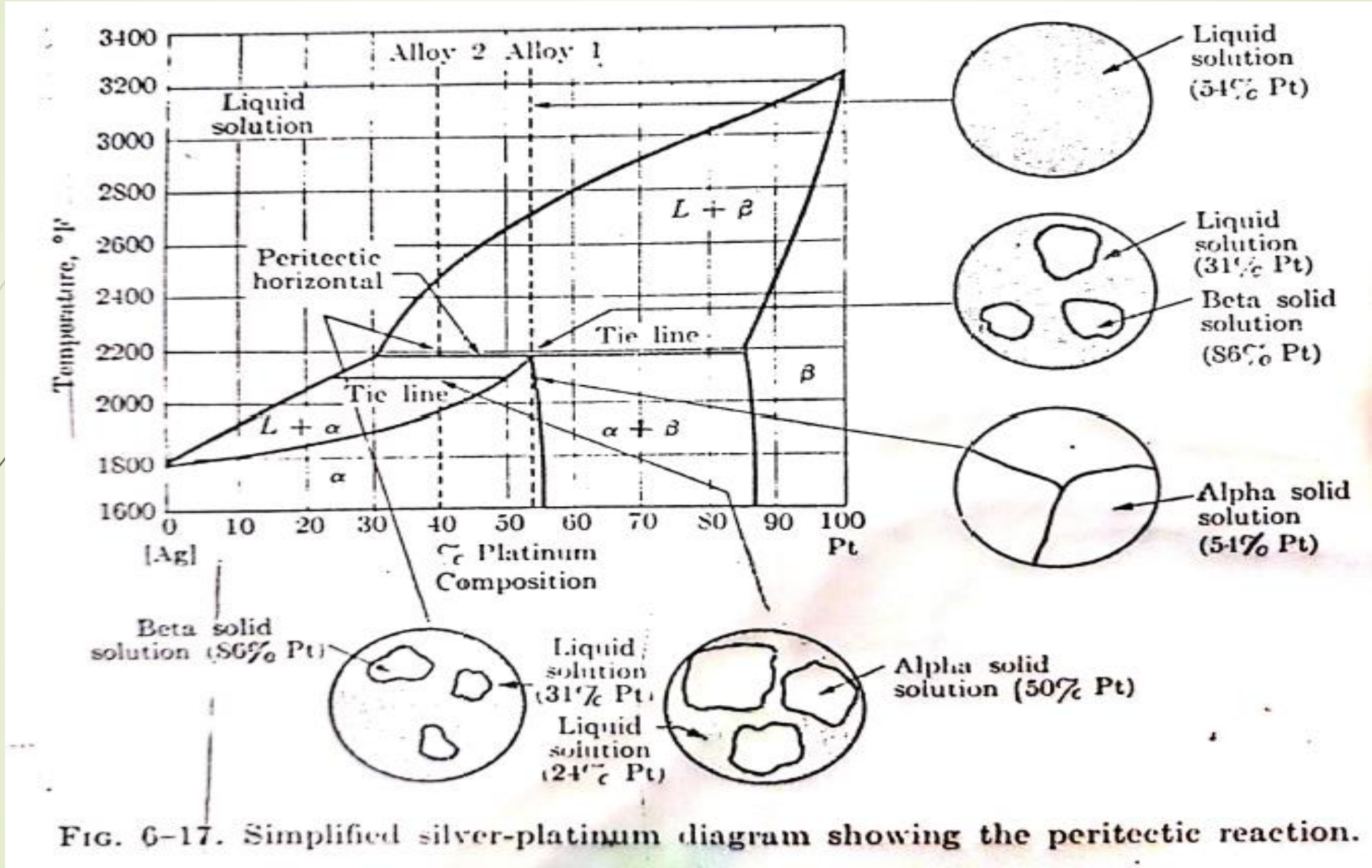

FIG. 6–17. Simplified silver-platinum diagram showing the peritectic reaction.

Eutectic	$L \rightarrow \alpha + \beta$	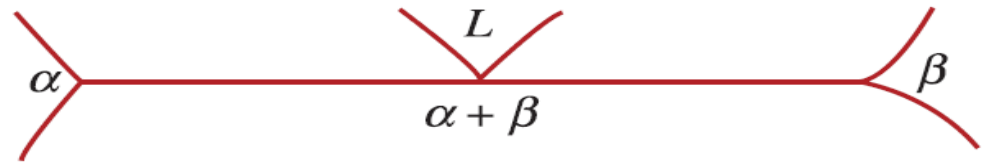
Peritectic	$\alpha + L \rightarrow \beta$	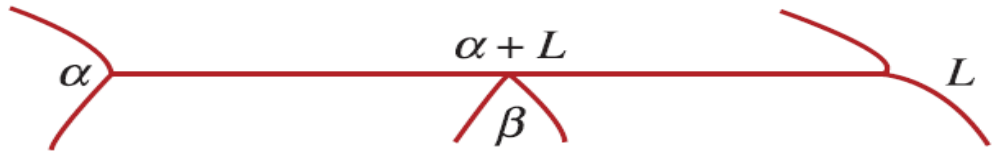
Monotectic	$L_1 \rightarrow L_2 + \alpha$	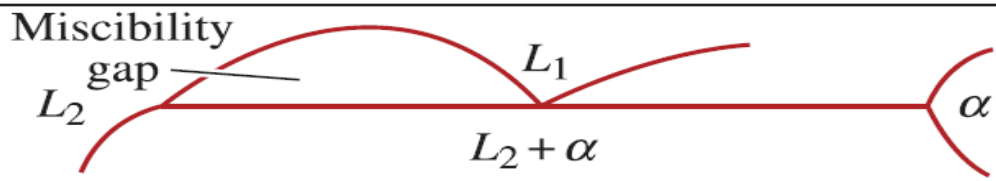
Eutectoid	$\gamma \rightarrow \alpha + \beta$	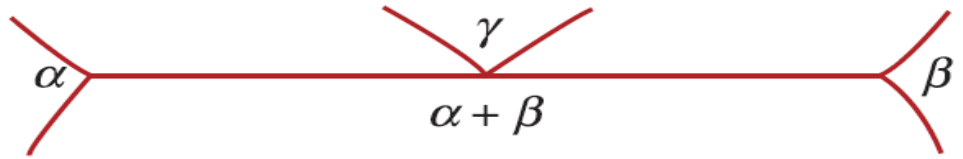
Peritectoid	$\alpha + \beta \rightarrow \gamma$	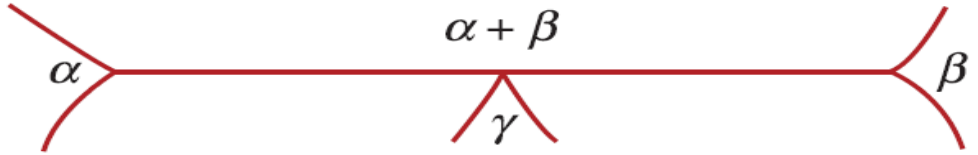

Figure 11-4 The five most important three-phase reactions in binary phase diagrams.

دیاگرام اهن کربن

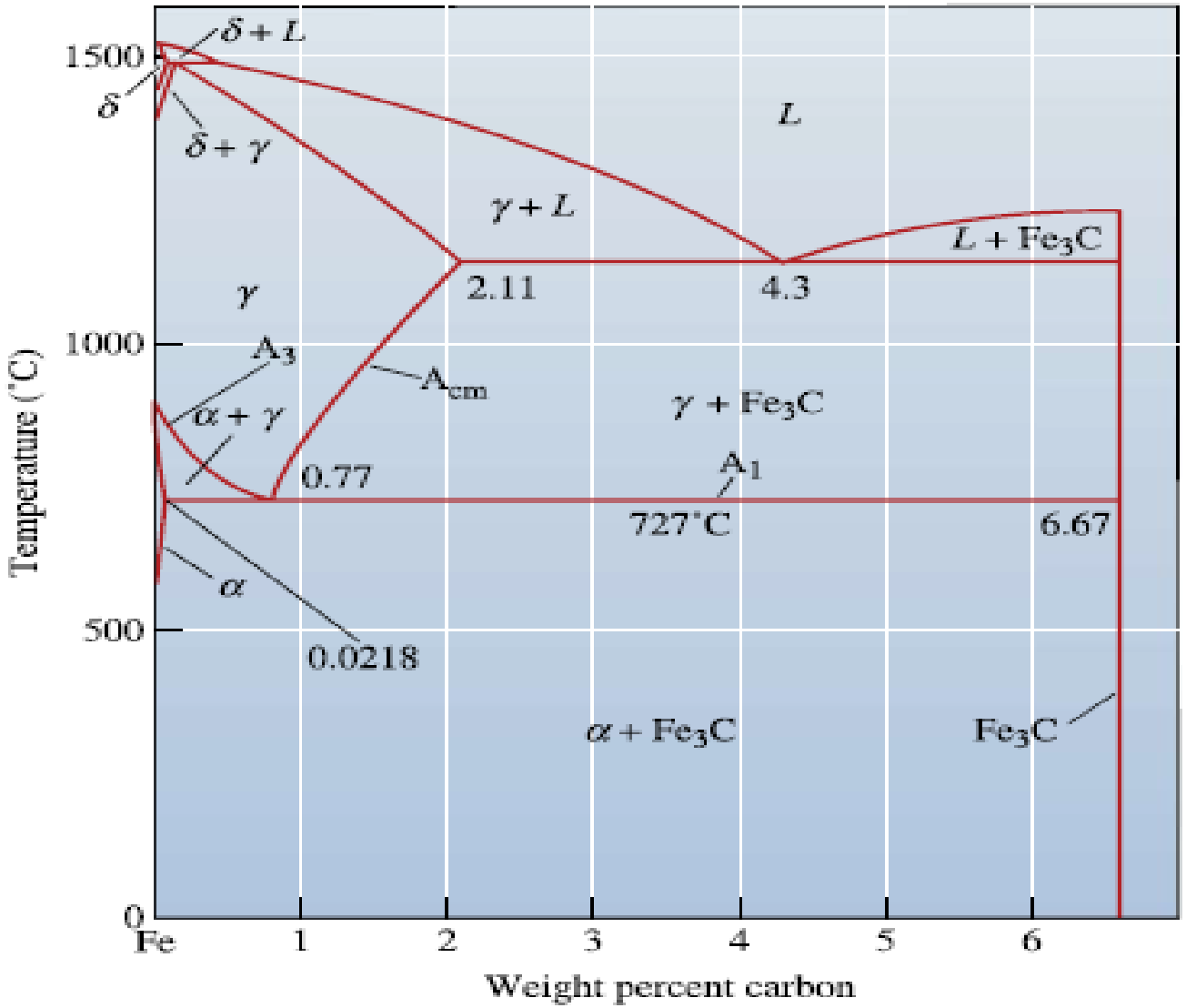

Figure 12-14 The Fe-Fe_3C phase diagram (a portion of the Fe-C diagram). The vertical line at 6.67% C is the stoichiometric compound Fe_3C.

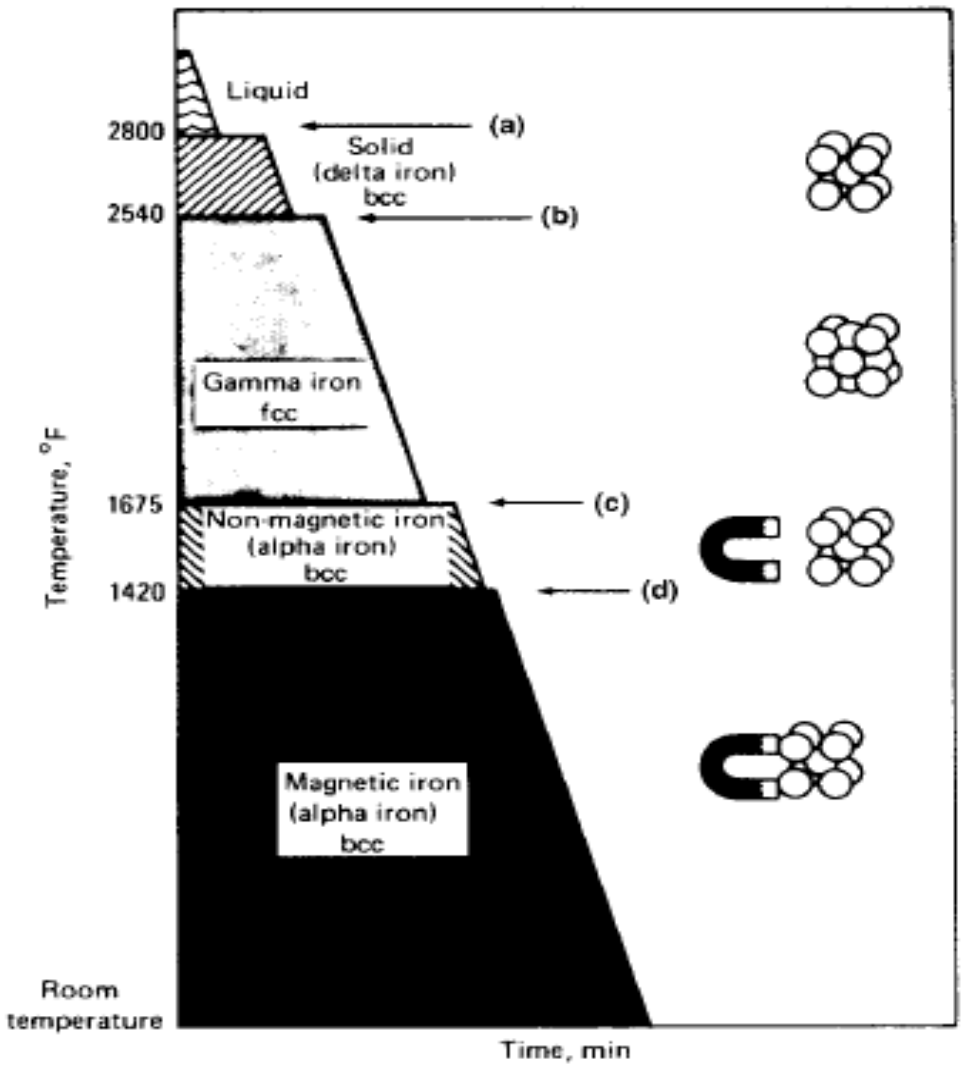

Fig. 1 Changes in pure iron as it cools from the molten state to room temperature. Source: Ref 3

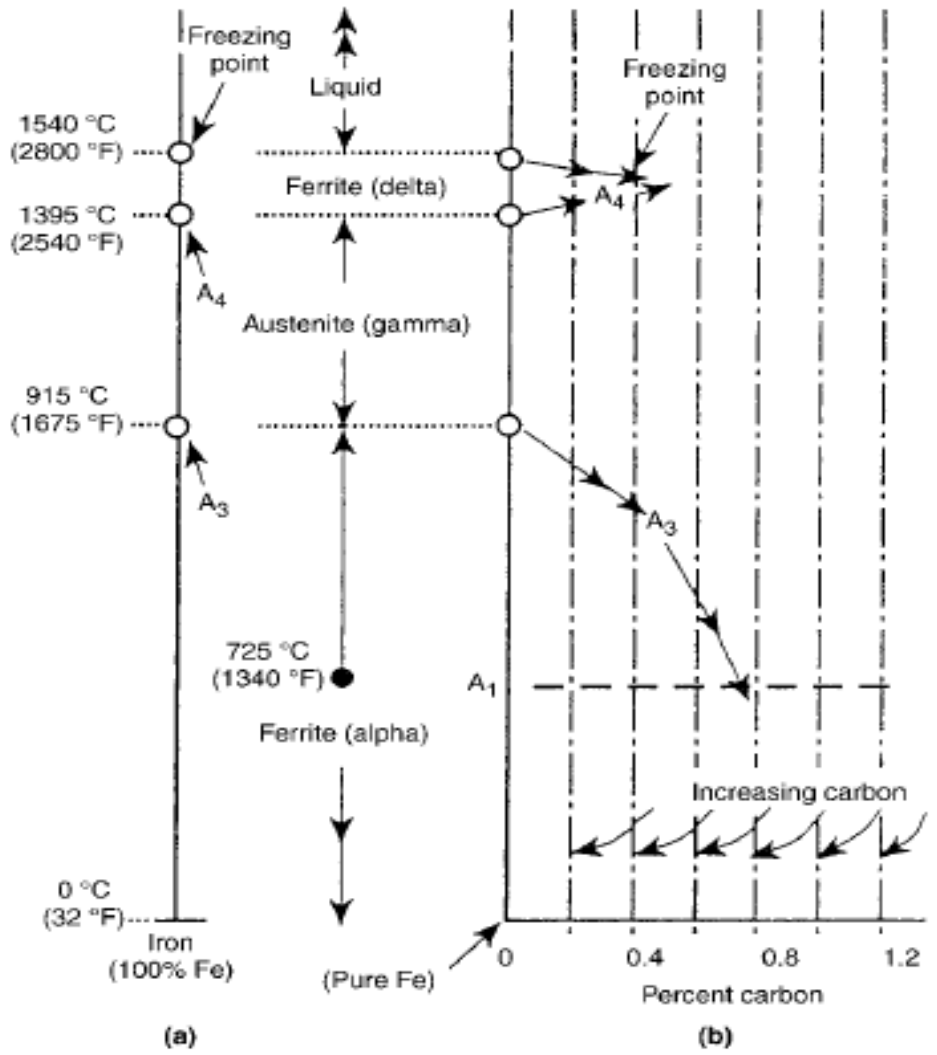

Fig. 3 Effects of carbon on the characteristics of commercially pure iron. (a) Constitutional diagram for pure iron. (b) Initial effects of carbon on the principal thermal points of pure iron. Source: Ref 3

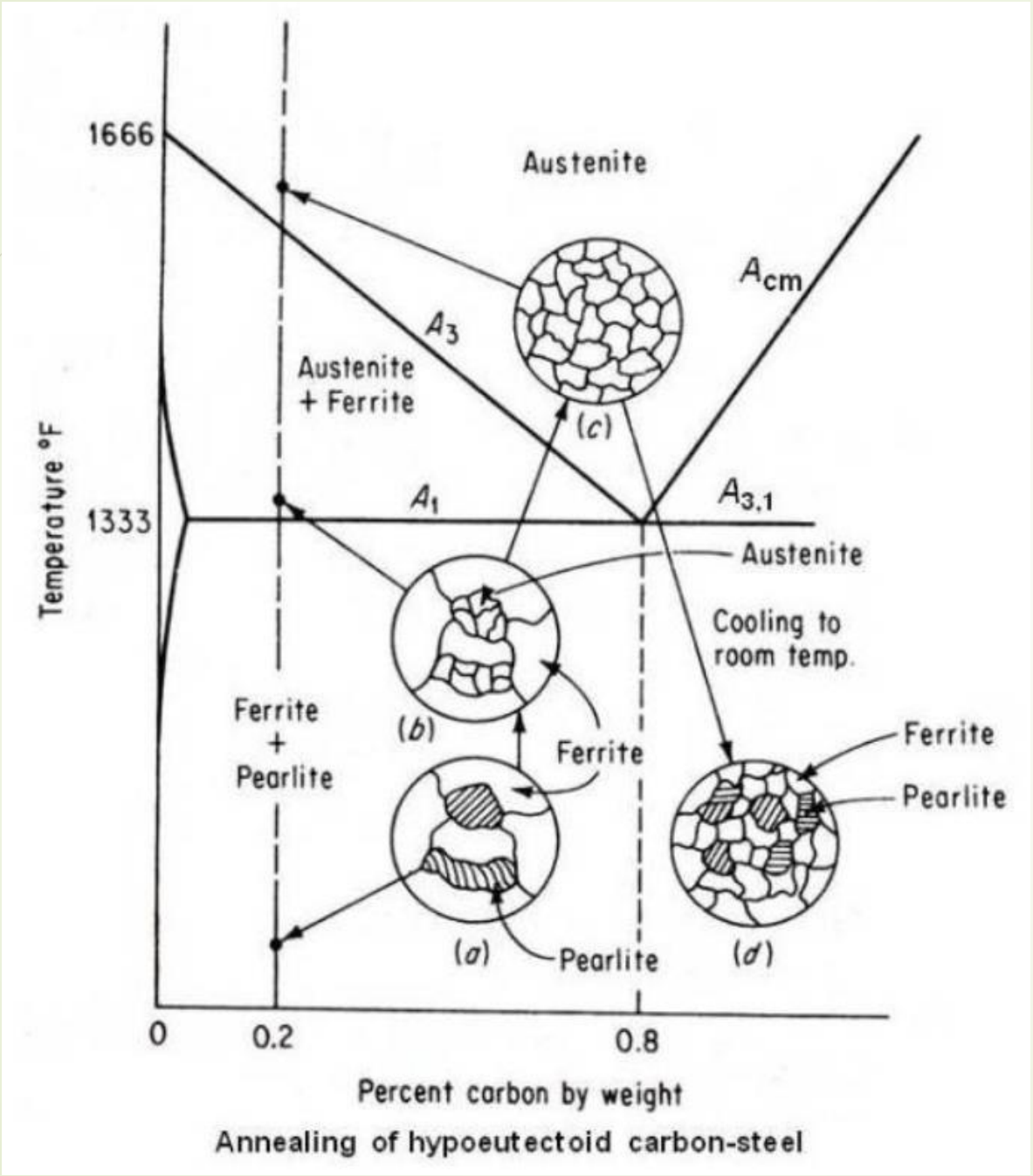

Annealing of hypoeutectoid carbon-steel

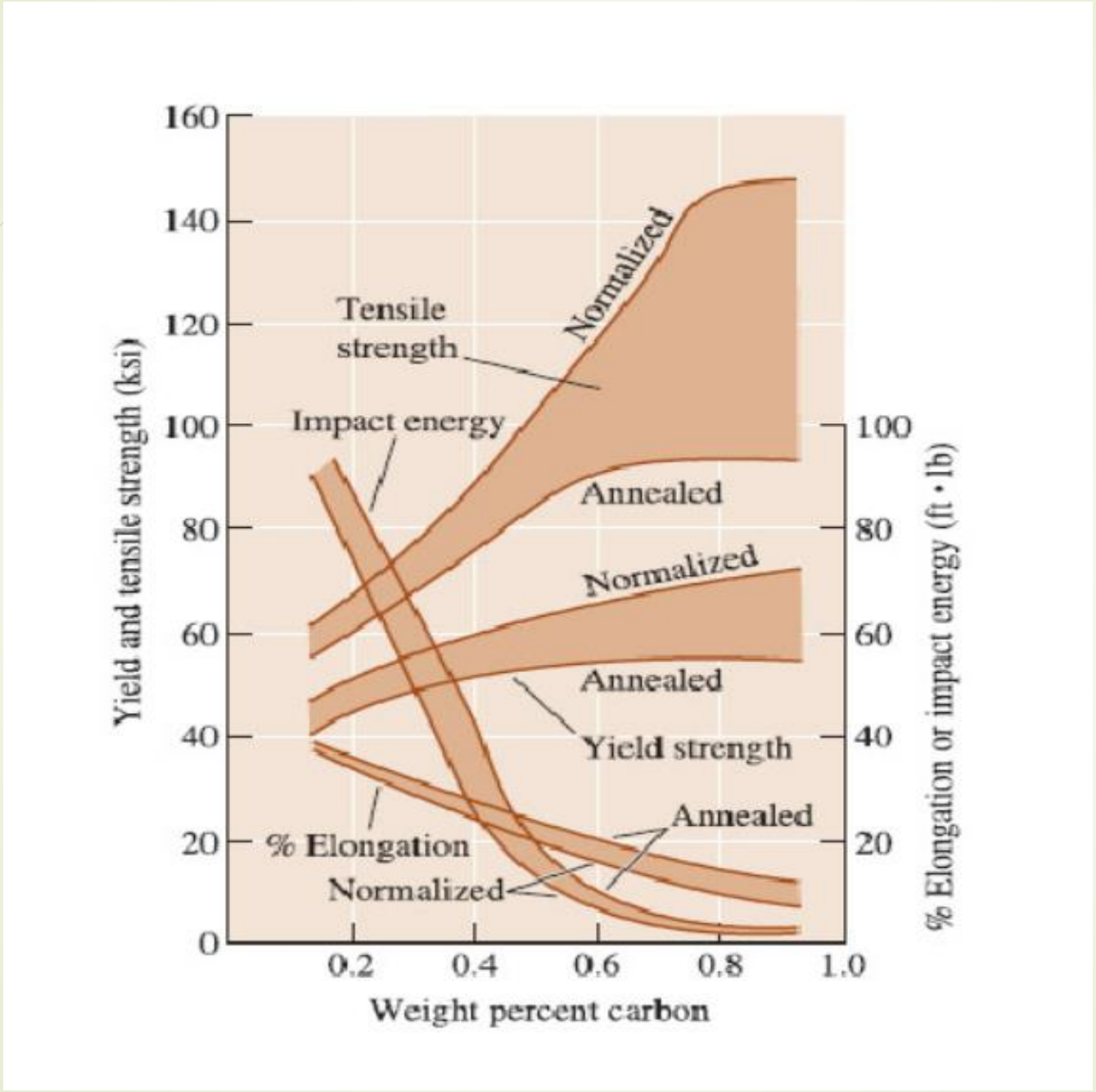
160
140
120
100
80
60
40
20
0
0.2
0.4
0.6
0.8
1.0
Yield and tensile strength (ksi)
% Elongation or impact energy (ft • lb)
Weight percent carbon
Tensile strength
Impact energy
% Elongation
Yield strength
Normalized
Annealed
Normalized
Annealed
Annealed
Normalized

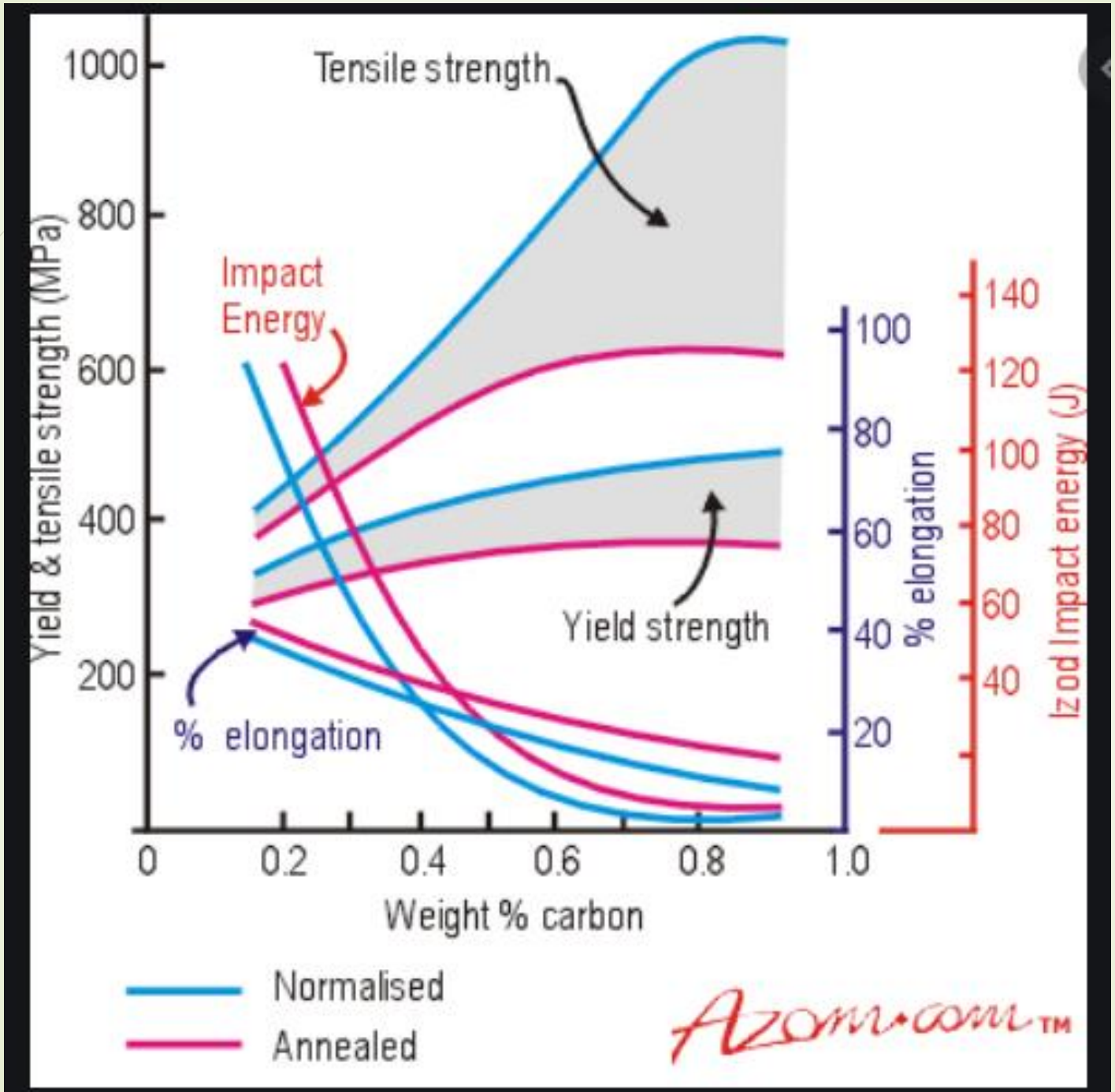
Tensile strength
Impact Energy
Yield strength
% elongation
Yield & tensile strength (MPa)
% elongation
Izod Impact energy (J)
Weight % carbon
1000
800
600
400
200
100
80
60
40
20
140
120
100
80
60
40
0
0.2
0.4
0.6
0.8
1.0
Normalised
Annealed
Azom.com™

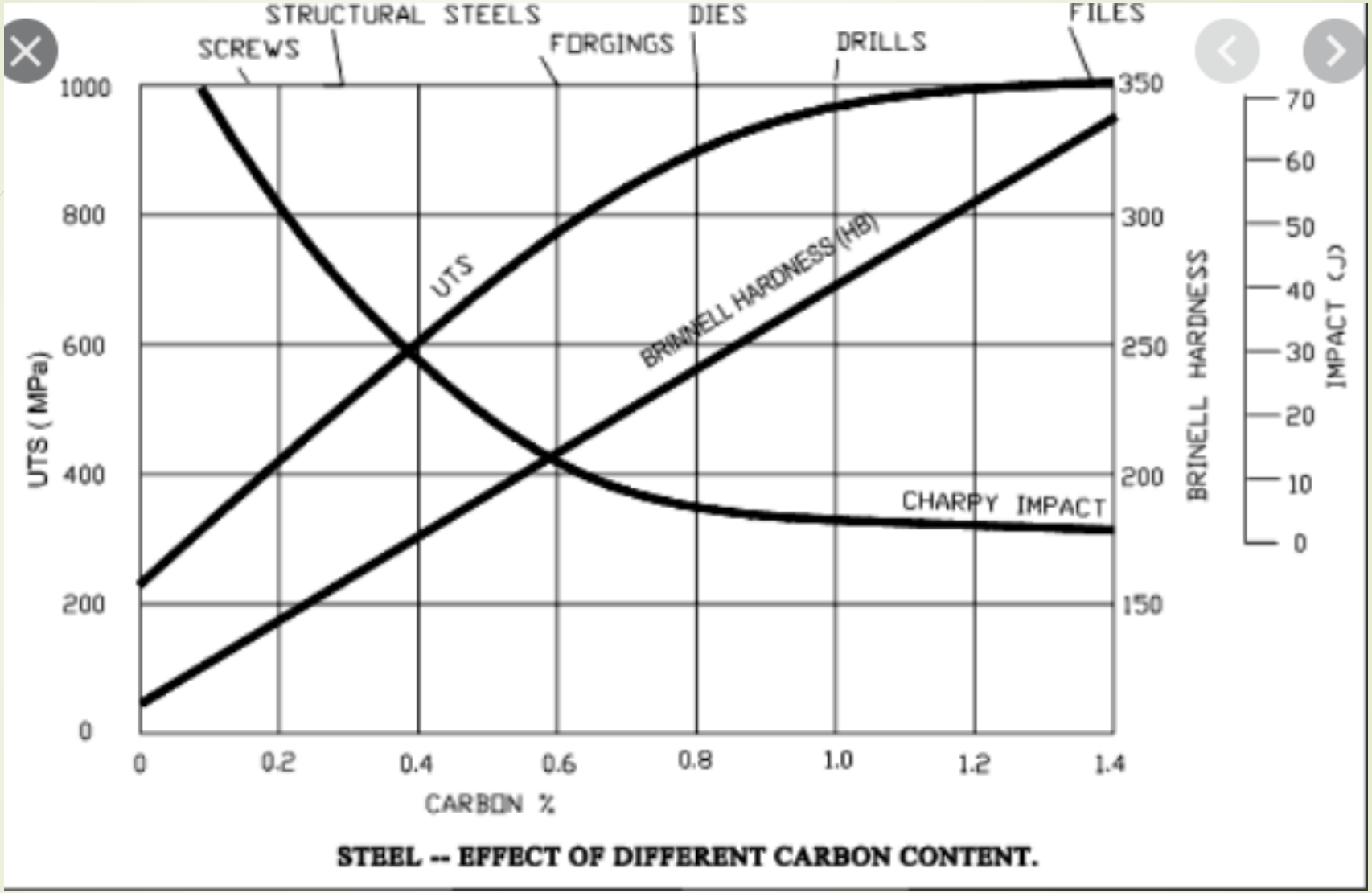

STEEL -- EFFECT OF DIFFERENT CARBON CONTENT.

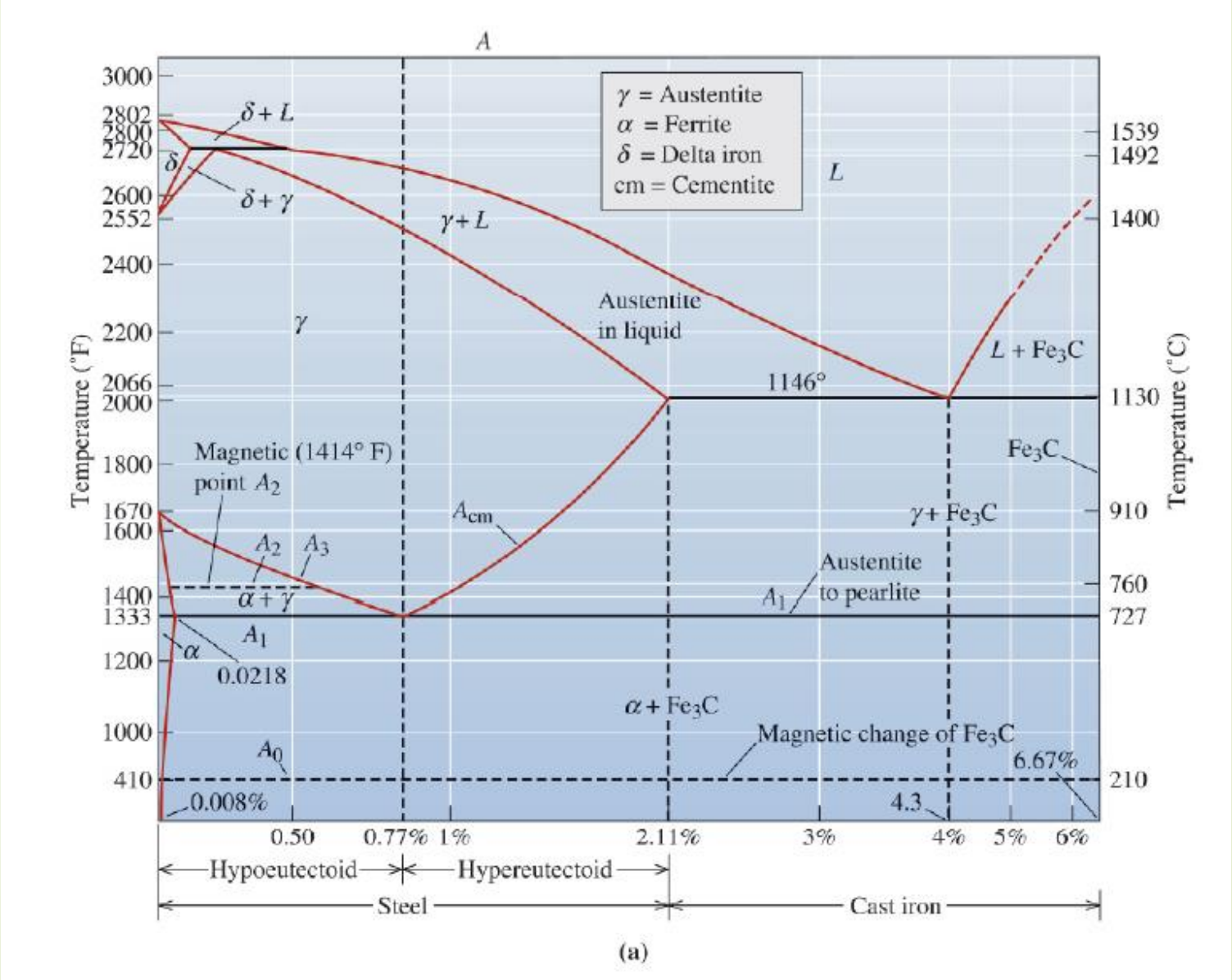
A
γ = Austentite
α = Ferrite
δ = Delta iron
cm = Cementite
L
δ + L
δ
δ + γ
γ + L
γ
Austentite in liquid
L + Fe3C
1146°
Magnetic (1414° F) point A2
Acm
A2
A3
α + γ
A1
α
0.0218
Austentite to pearlite
γ + Fe3C
Fe3C
α + Fe3C
Magnetic change of Fe3C
A0
0.008%
6.67%
4.3
3000
2802
2800
2720
2600
2552
2400
2200
2066
2000
1800
1670
1600
1400
1333
1200
1000
410
1539
1492
1400
1130
910
760
727
210
Temperature (°F)
Temperature (°C)
0.50
0.77%
1%
2.11%
3%
4%
5%
6%
Hypoeutectoid
Hypereutectoid
Steel
Cast iron
(a)

Solid Solutions

Iron goes through two allotropic transformations (Chapter 3) during heating or cooling. Immediately after solidification, iron forms a BCC structure called δ-ferrite. On further cooling, the iron transforms to a FCC structure called γ, or **austenite**. Finally, iron transforms back to the BCC structure at lower temperatures; this structure is called α, or **ferrite**. Both of the ferrites (α and δ) and the austenite are solid solutions of interstitial carbon atoms in iron. Normally, when no specific reference is made, the term ferrite refers to the α ferrite, since this is the phase we encounter more often during the heat treatment of steels. Certain ceramic materials used in magnetic applications are also known as ferrites (Chapter 20) but are not related to the ferrite phase in the Fe-Fe_3C system.

Because interstitial holes in the FCC crystal structure are somewhat larger than the holes in the BCC crystal structure, a greater number of carbon atoms can be accommodated in FCC iron. Thus, the maximum solubility of carbon in austenite is 2.11% C, whereas the maximum solubility of carbon in BCC iron is much lower (i.e., ~0.0218% C in α and 0.09% C in δ). The solid solutions of carbon in iron are relatively soft and ductile, but are stronger than pure iron due to solid-solution strengthening by the carbon.

Understanding of Fe –C Phase Equilibrium - 1946

Tool Available at the time:

*X-ray Diffraction

*Optical Metallography

*Thermocouples

Delta – BCC

Austenite – FCC

Ferrite – BCC

Cementite - Orthorhombic

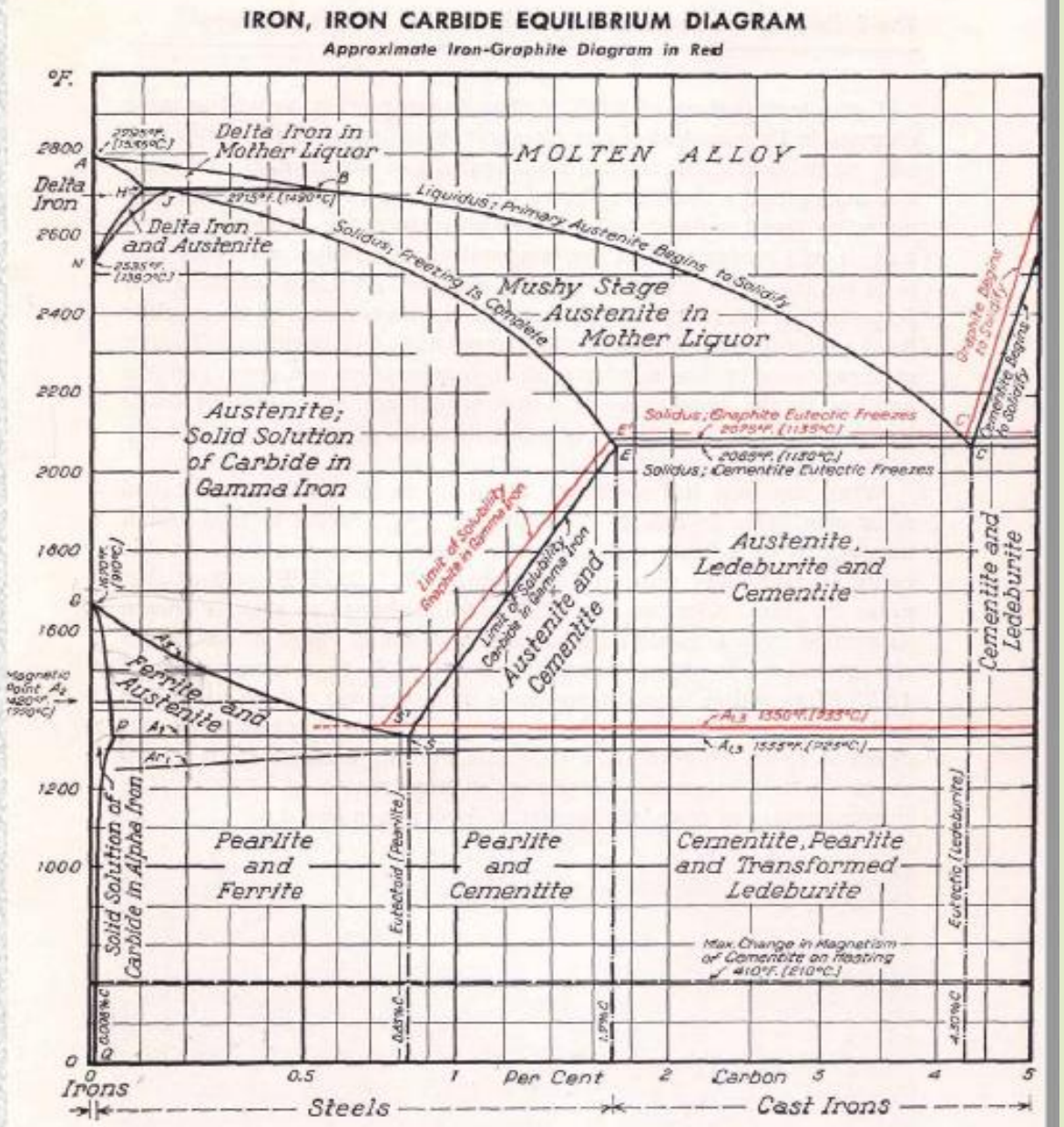

Fig. 3—The Iron-Carbon Equilibrium Diagram (Metal Progress July, 1946)

دیاگرام اهن-کربن واکنش یوتکتیک ویوتکتوئید

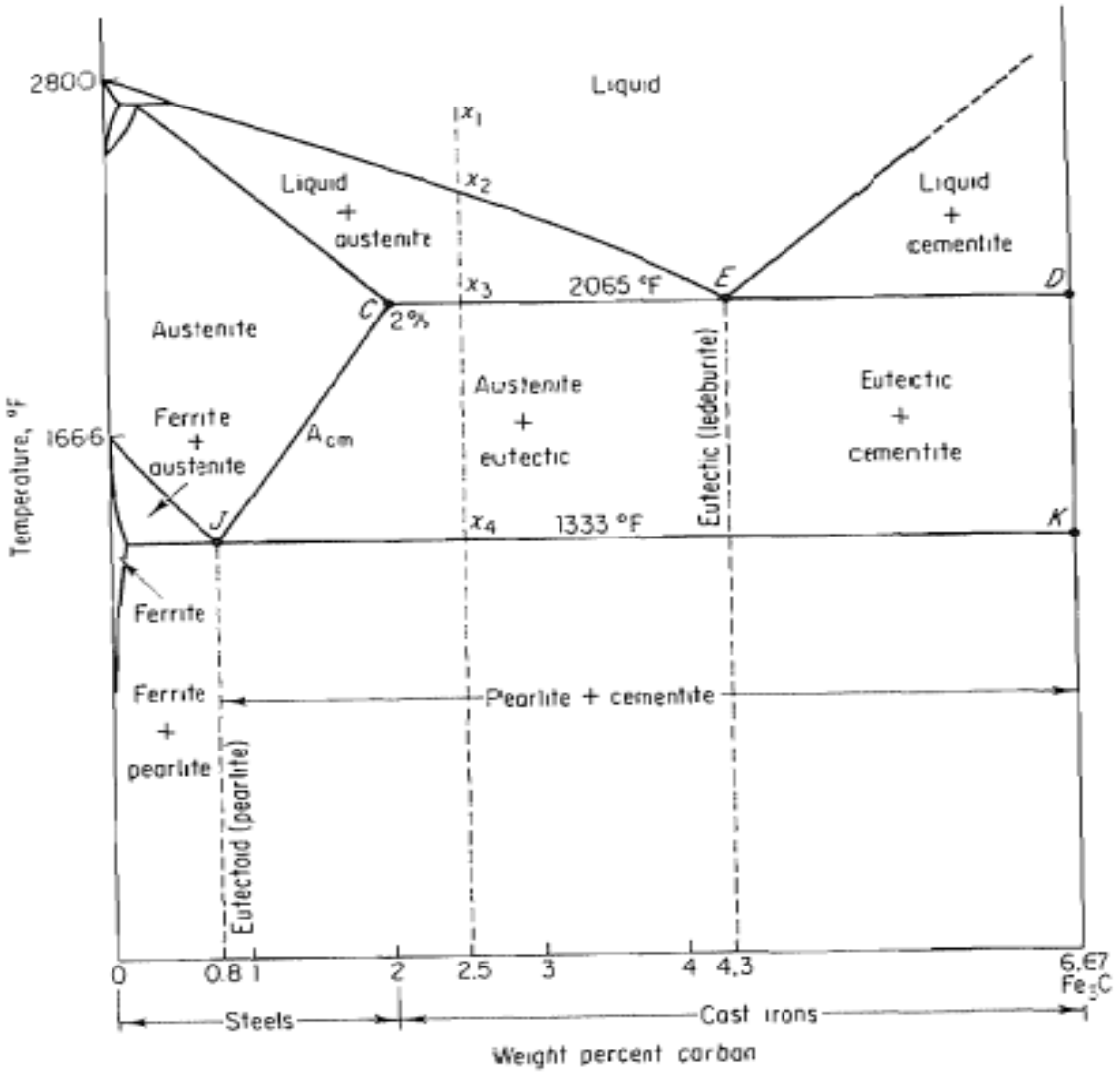

Fig. 11·1 The metastable iron–iron carbide phase diagram.

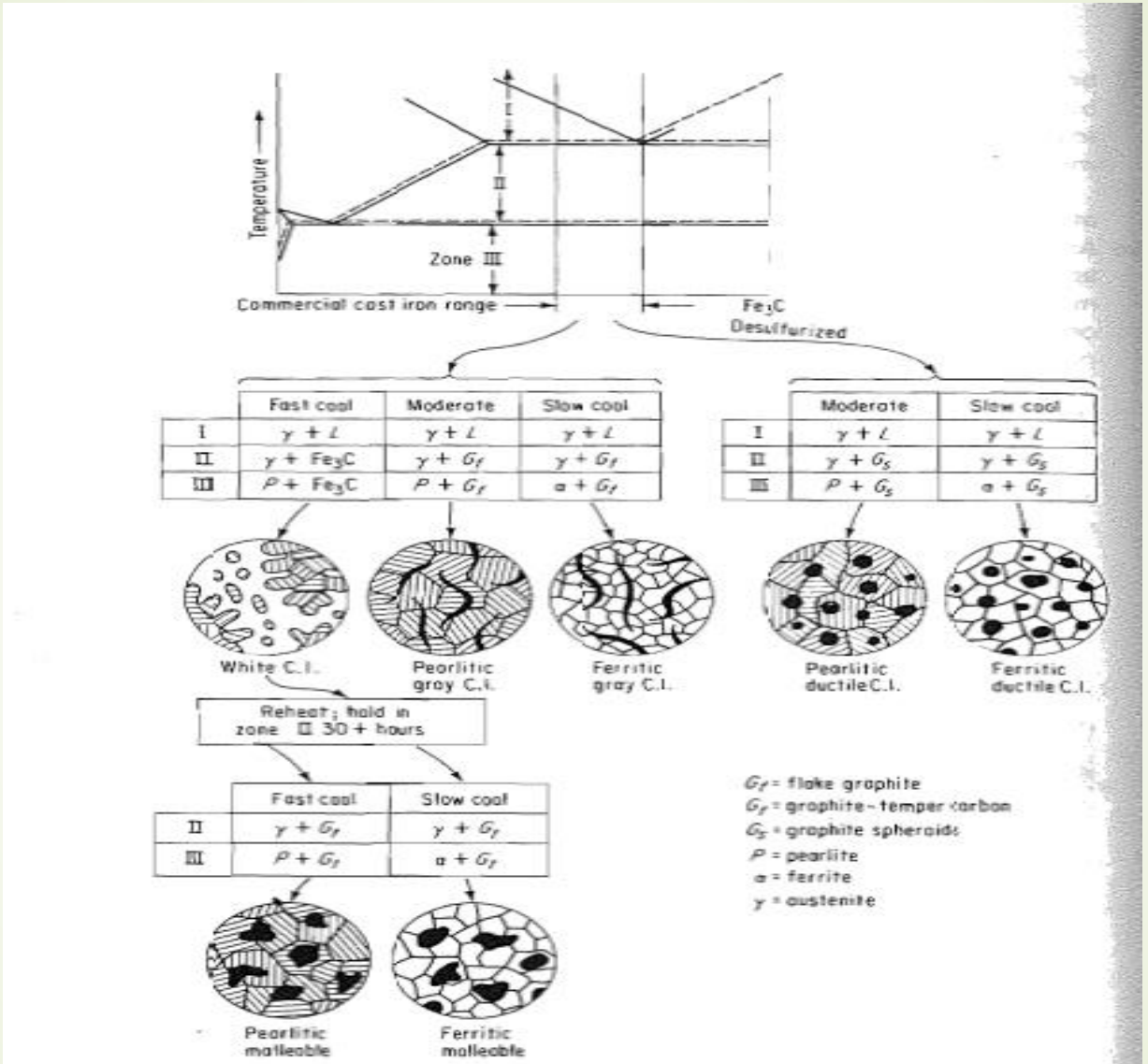

Fig. 11-24 Summary of cast-iron microstructures and the phases coexisting at various temperatures. (From Moffatt, Pearsall, and Wulff, "The Structure and Properties of Materials," John Wiley & Sons, Inc., New York, 1964.)

ریزساختار فولاد هیپو یوتکتیک وهایپر یوتکتیک

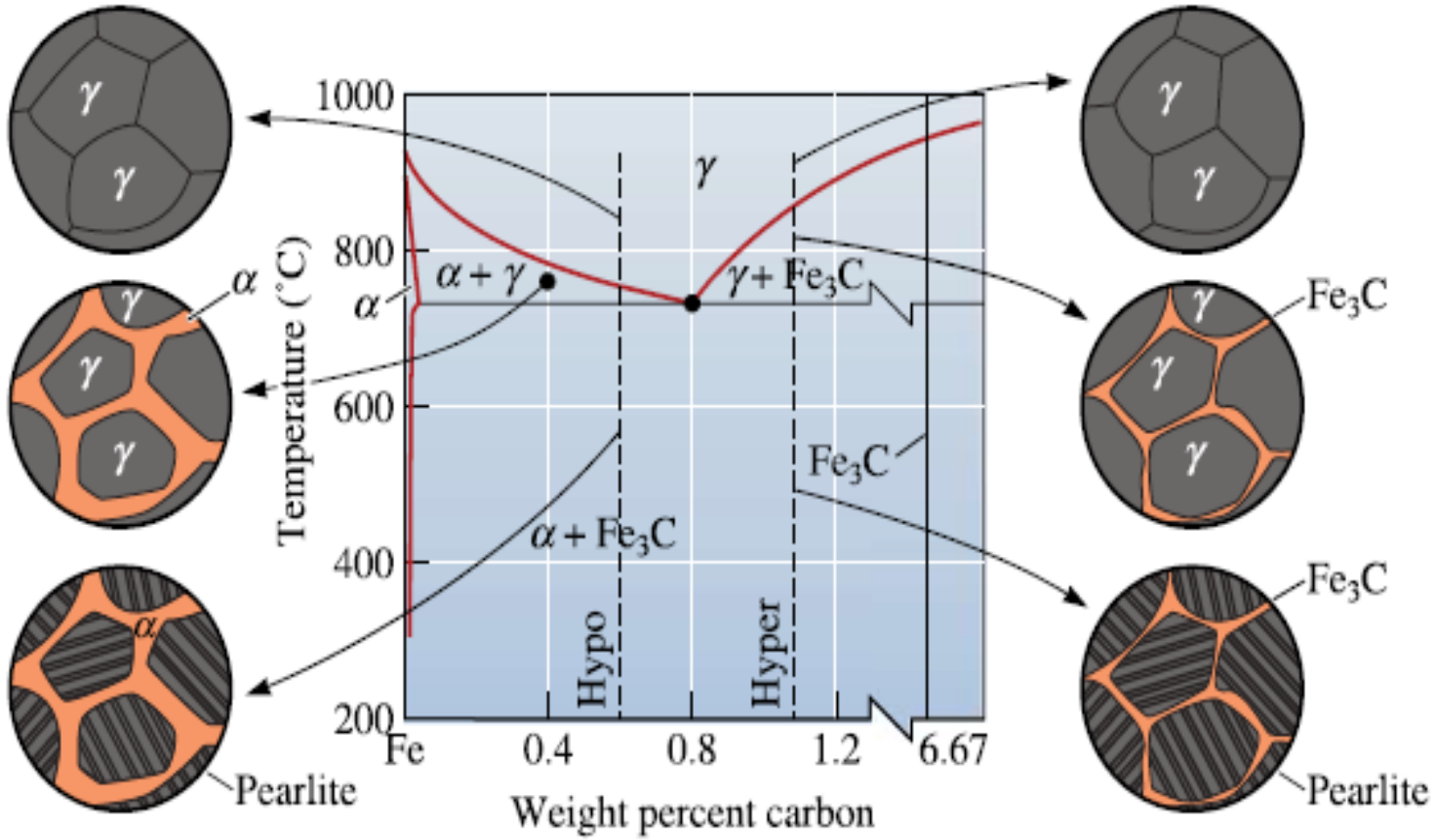

Figure 12-16 The evolution of the microstructure of hypoeutectoid and hypereutectoid steels during cooling, in relationship to the Fe-Fe_3C phase diagram.

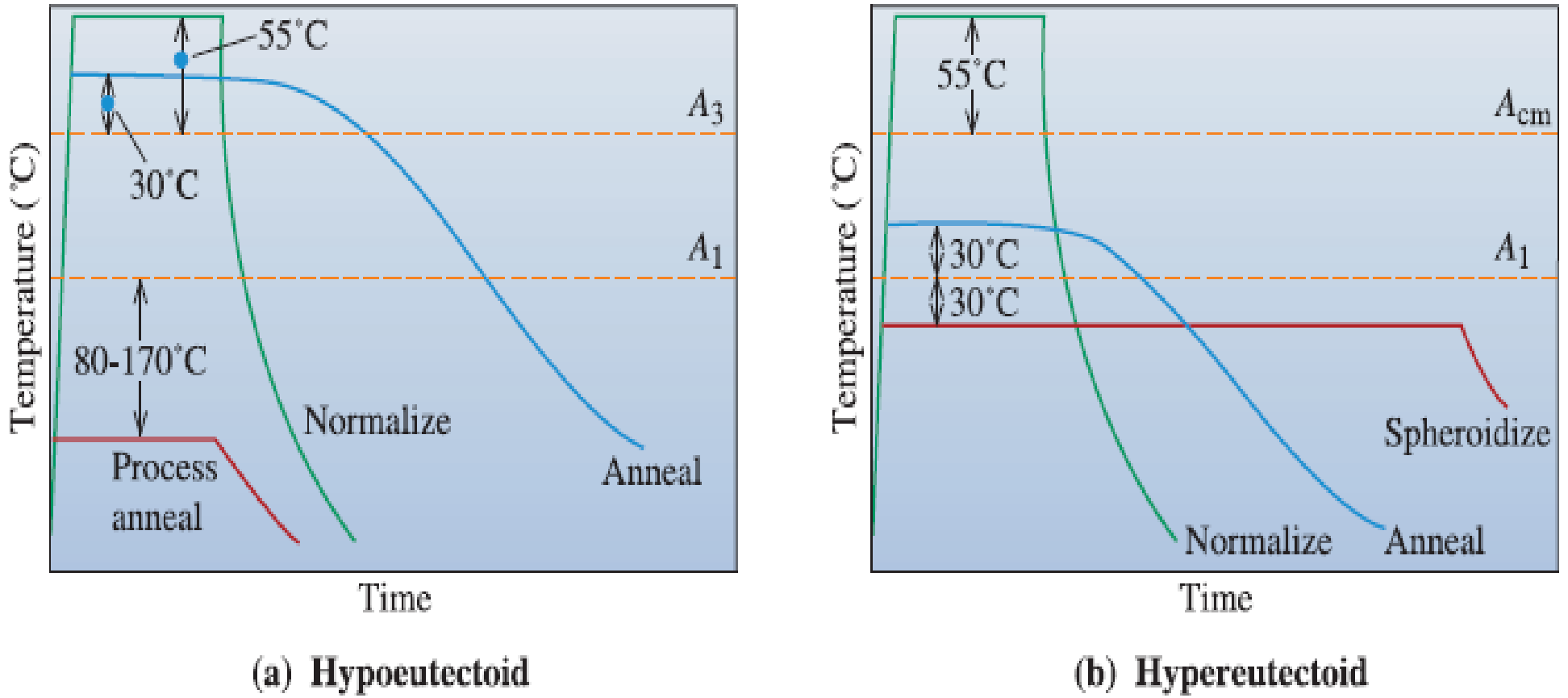

Figure 13-3 Schematic summary of the simple heat treatments for (a) hypoeutectoid steels and (b) hypereutectoid steels.

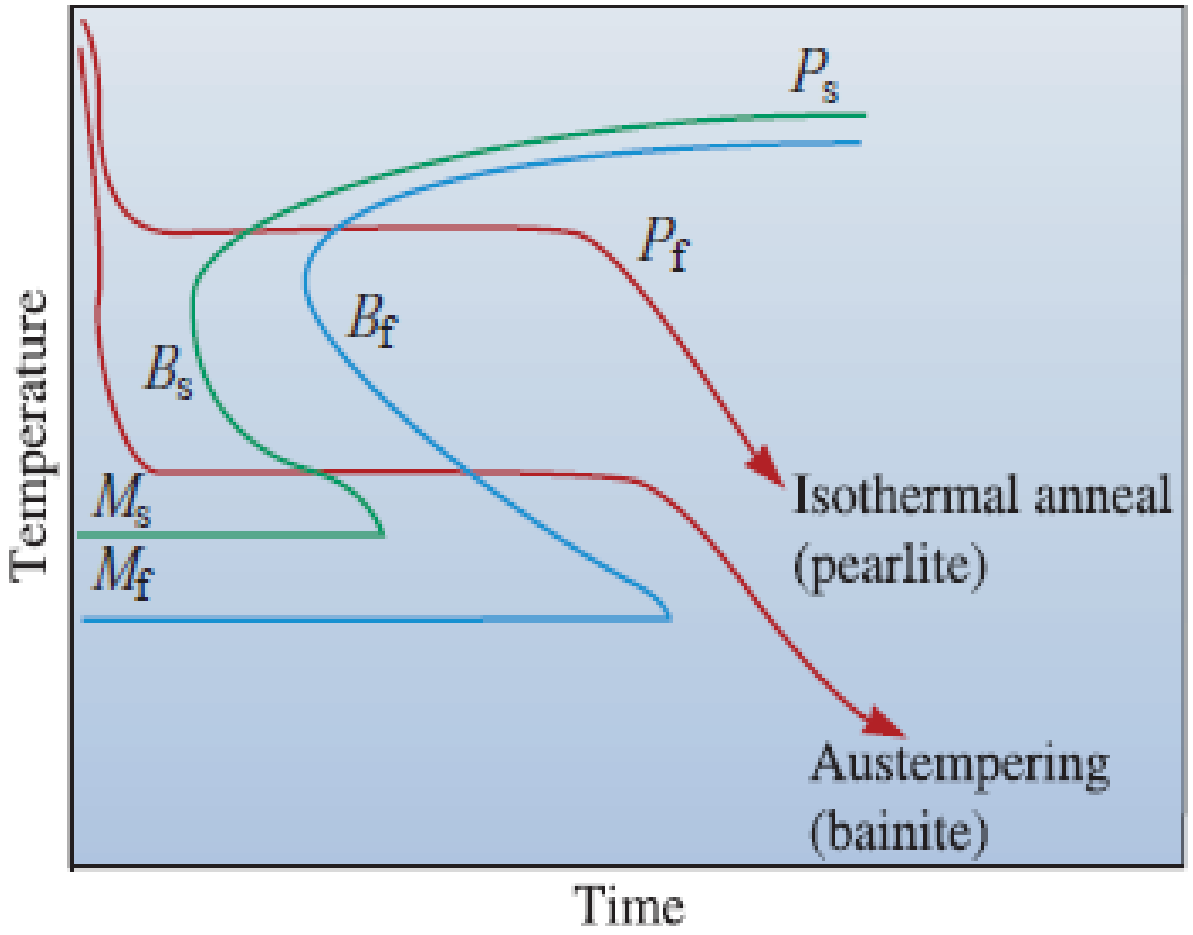

Figure 13-6 The austempering and isothermal anneal heat treatments in a 1080 steel.

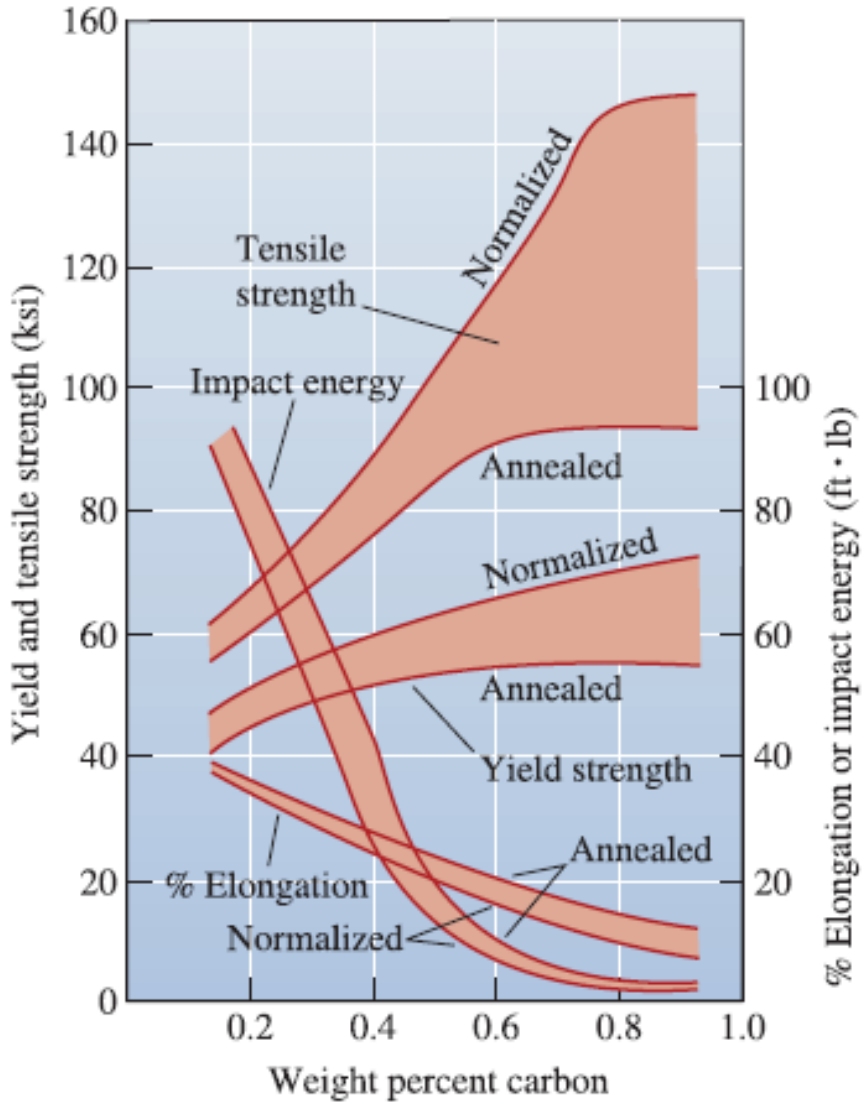

Figure 13-4
The effect of carbon and heat treatment on the properties of plain carbon steels.

دیاگرامTTT

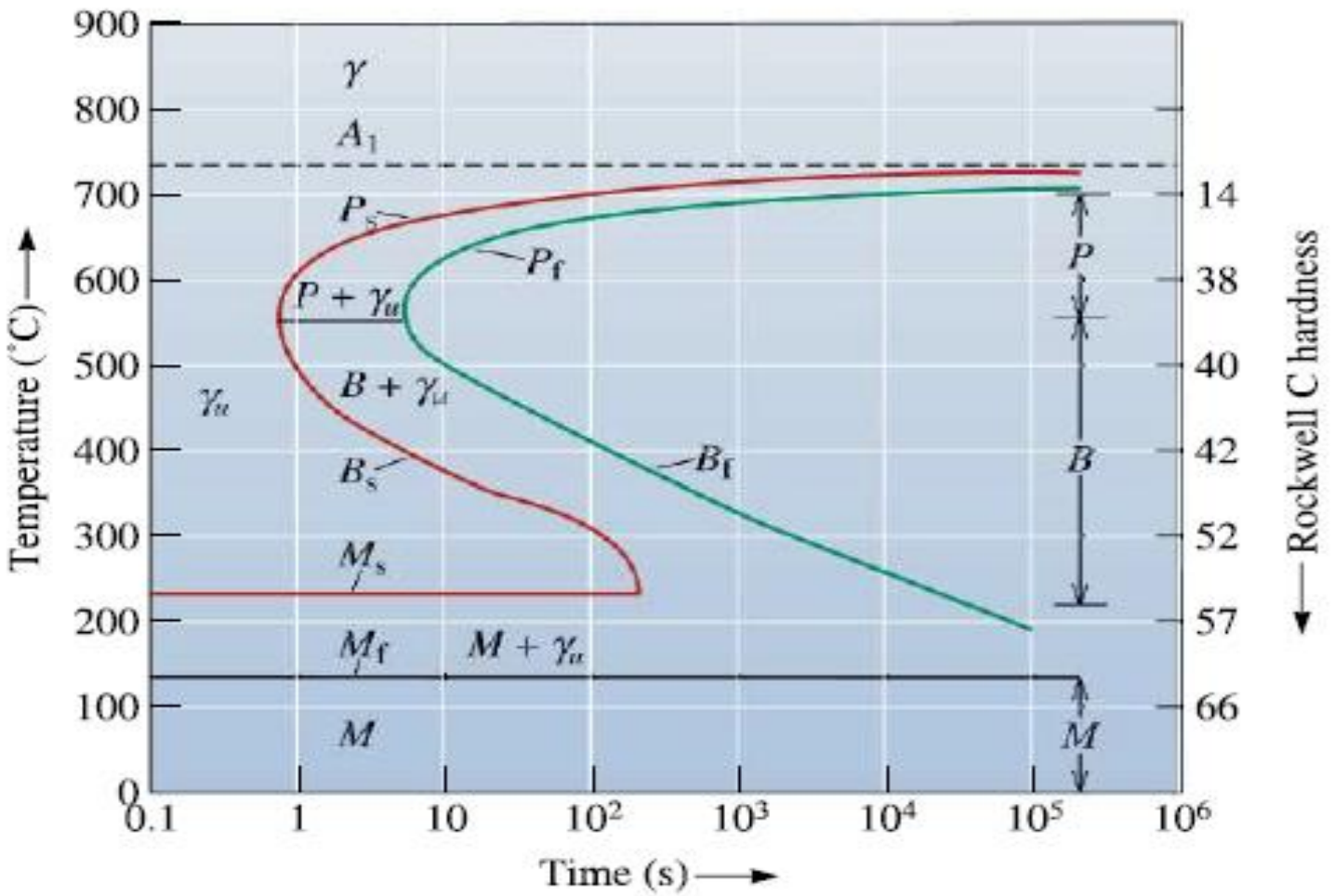

Figure 12-20 The time-temperature-transformation (TTT) diagram for a eutectoid steel, where P = Pearlite, B = Bainite, and M = Martensite. The subscripts "s" and "f" indicate the start and finish of a transformation. γ_u is unstable austenite.

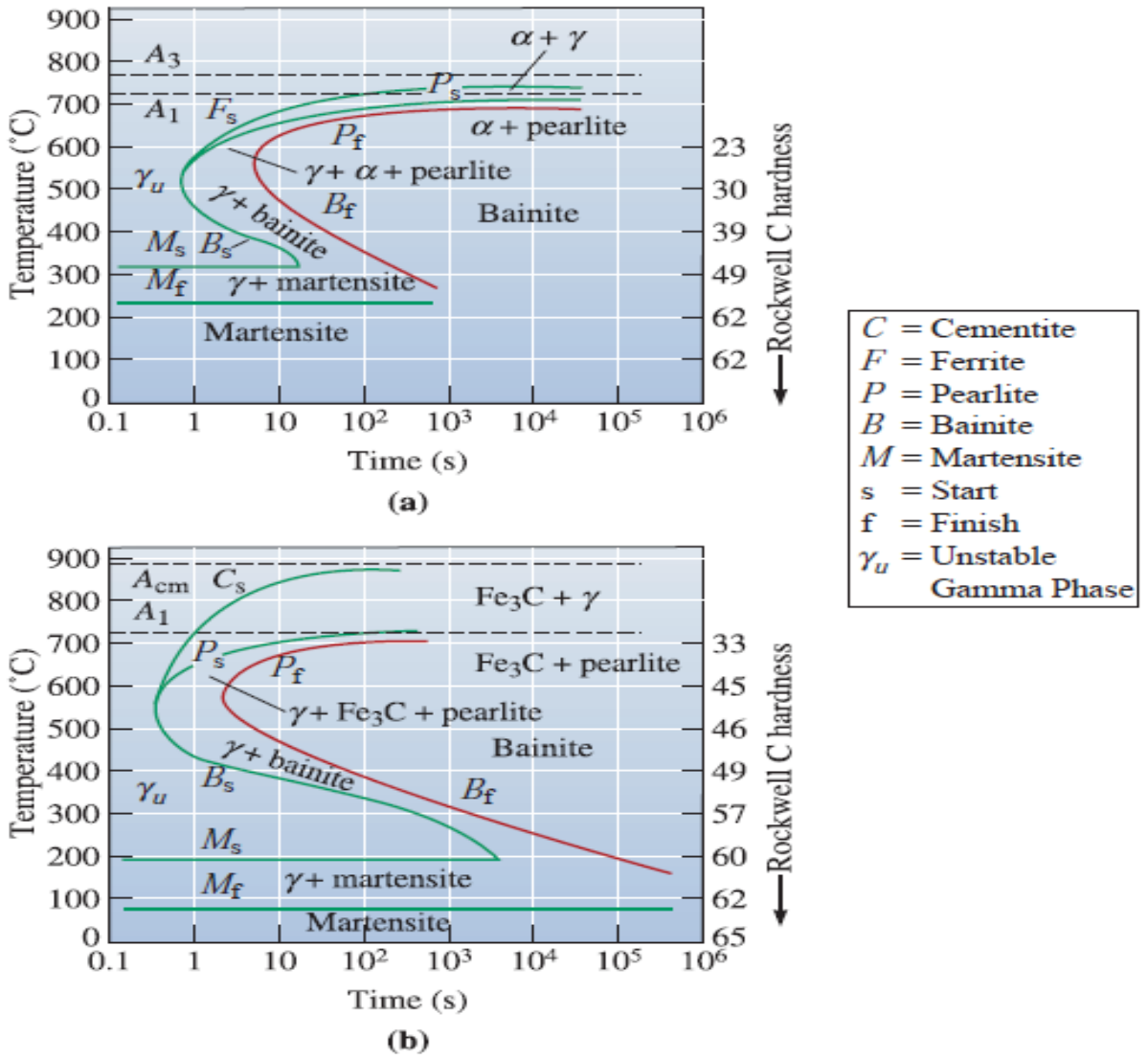

Figure 13-7 The TTT diagrams for (a) a 1050 and (b) a 10110 steel. Note γ_u = unstable austenite.

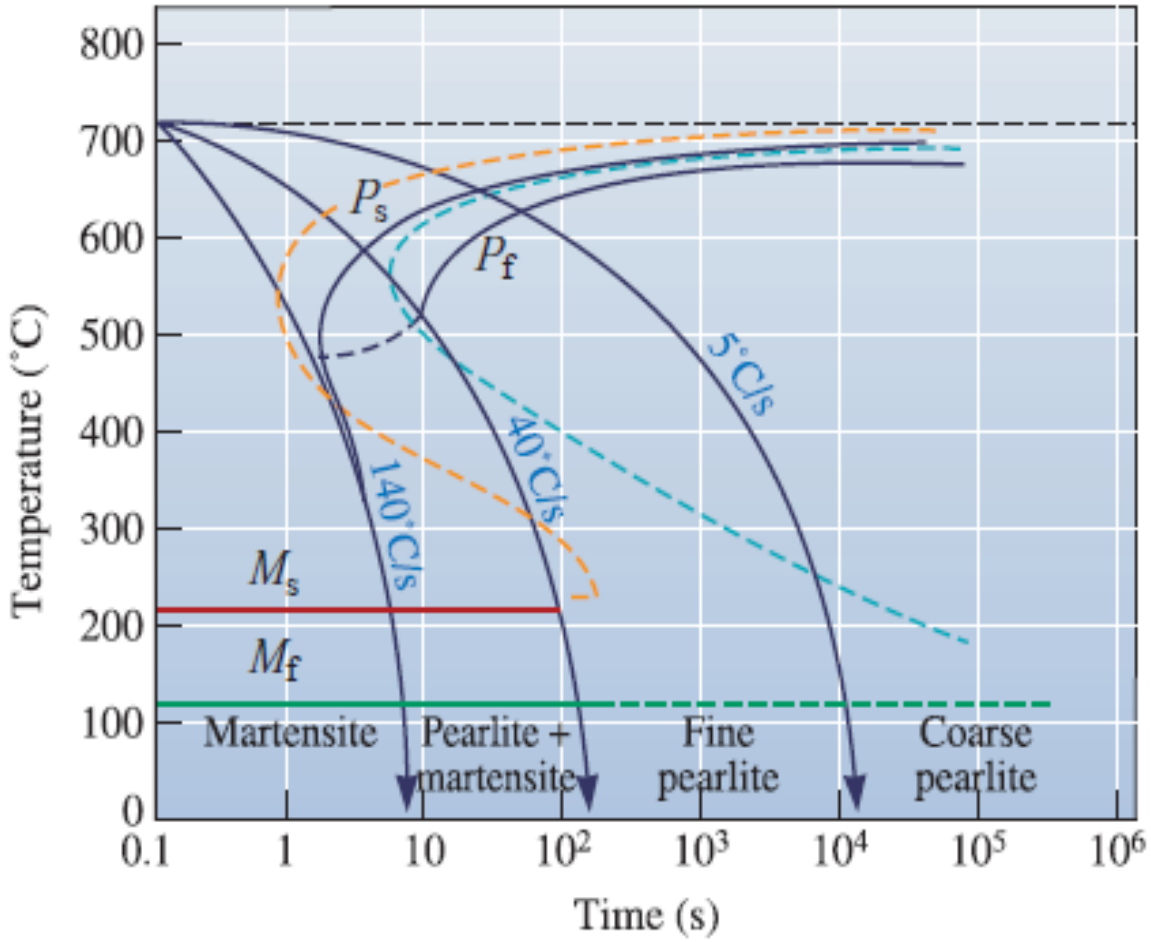

Figure 13-14 The CCT diagram (solid lines) for a 1080 steel compared with the TTT diagram (dashed lines).

دیاگرامTTT

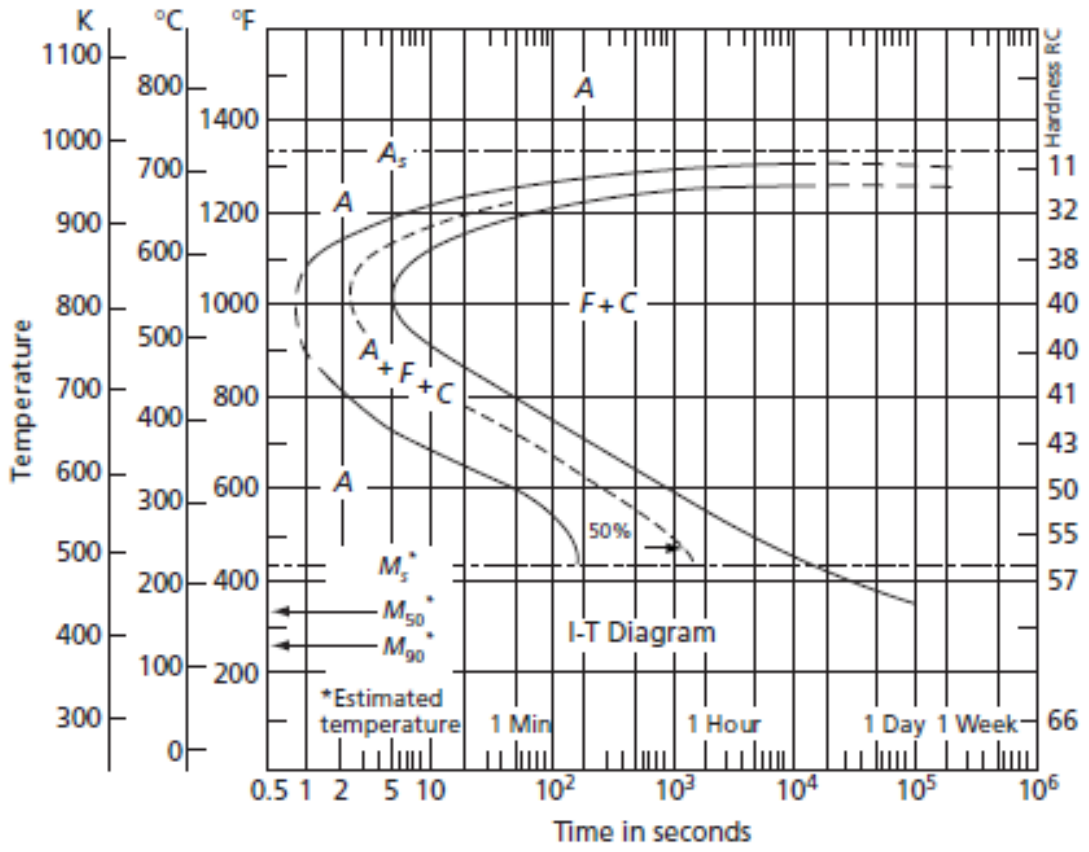

FIG. 18.30 The complete isothermal transformation diagram for an eutectoid steel. Notice that this steel is not a high-purity iron-carbon alloy, but a commercial steel (AISI 1080) containing 0.79 percent carbon and 0.76 percent manganese. The effect of the manganese will be discussed in Chapter 19. Note that the temperature is given in Centigrade, Fahrenheit, and Kelvin on the left and the hardness of the isothermally transformed specimens is shown on the right. In this figure A = austenite, F = ferrite, C = cementite, and M = martensite. (From *Atlas of Isothermal Transformation and Continuous Cooling Diagrams*, American Society for Metals, Metals Park, 1977. Reprinted with permission of AMS International (R). All rights reserved. www.asminternational.org)

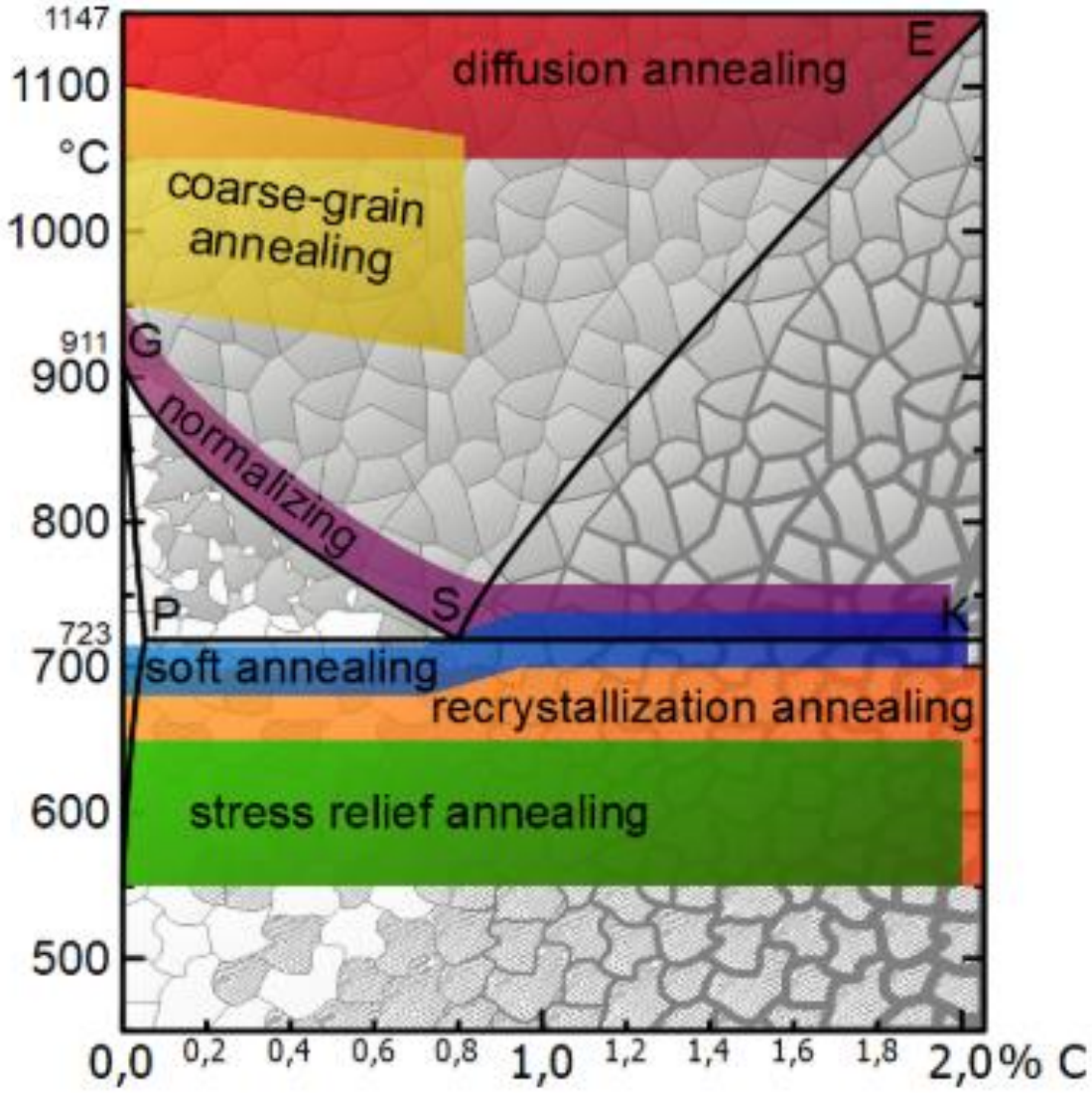

Figure: Temperature ranges of the heat treatment processes

عملیات حرارتی انیل –نرماله -کروی کردن

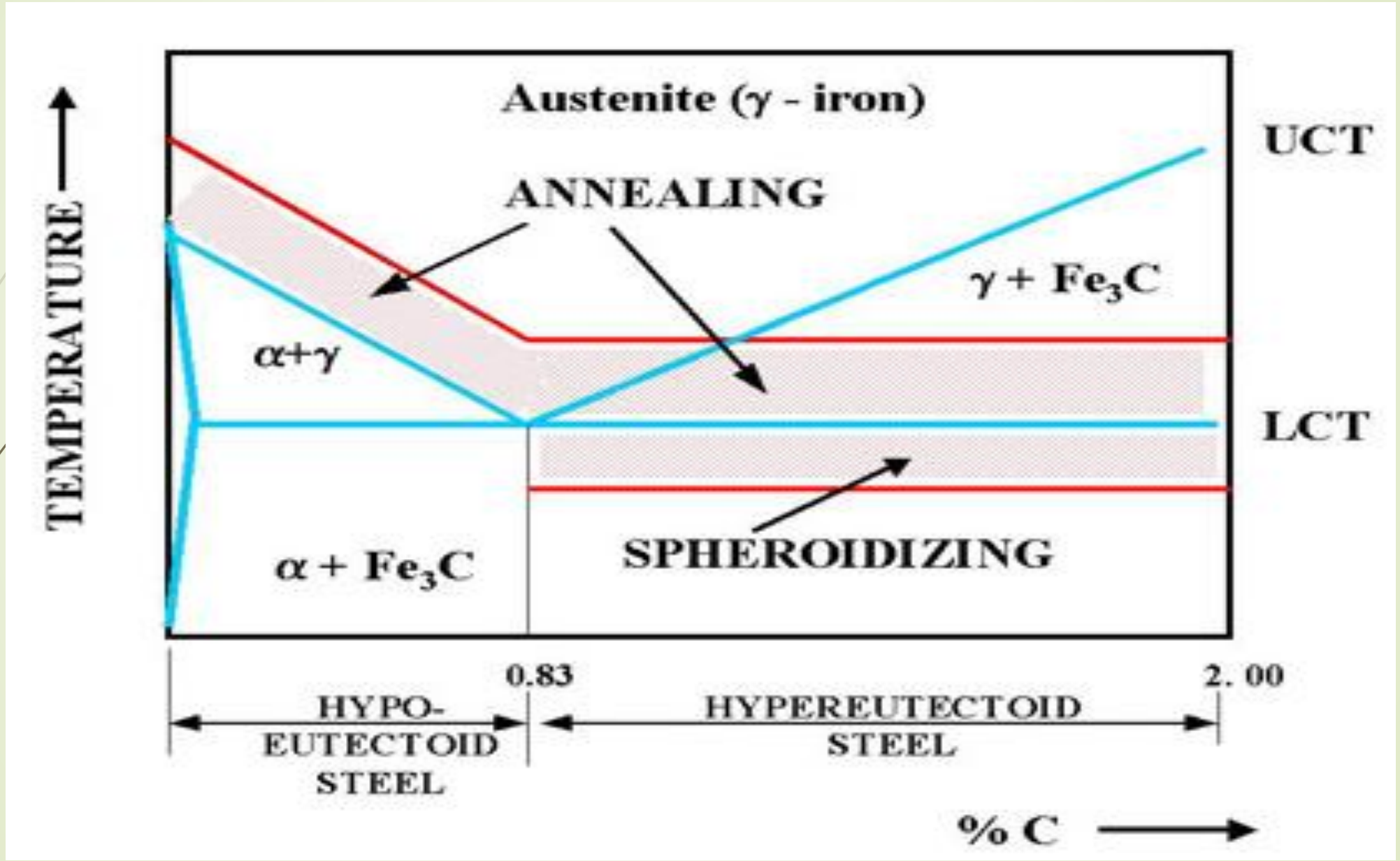

Temperature Regime of Steel Heat Treatment

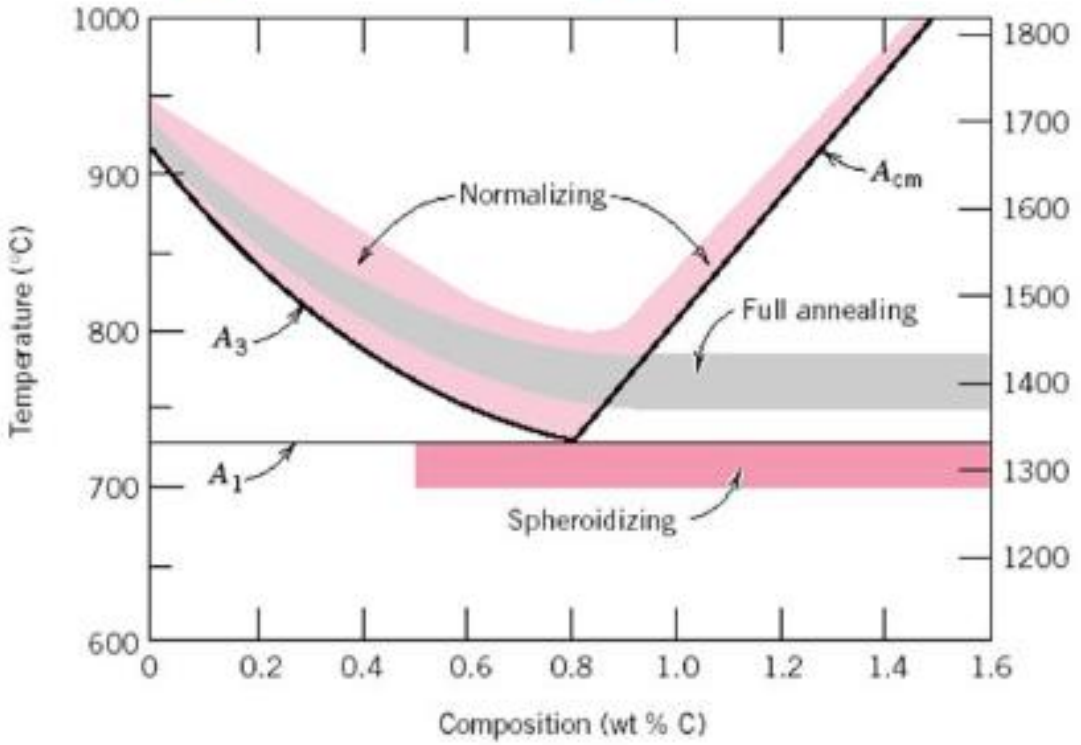

FIG. 11.9 The iron-iron carbide phase diagram in the vicinity of the eutectoid, indicating heat treating temperature ranges for the plain carbon steels.

- Most heat treating operations begin with heating the alloy into the austenitic phase field to dissolve the carbide in the iron
- Steel heat treating practice rarely involves the use of temperatures above 1040°C (1900°F)

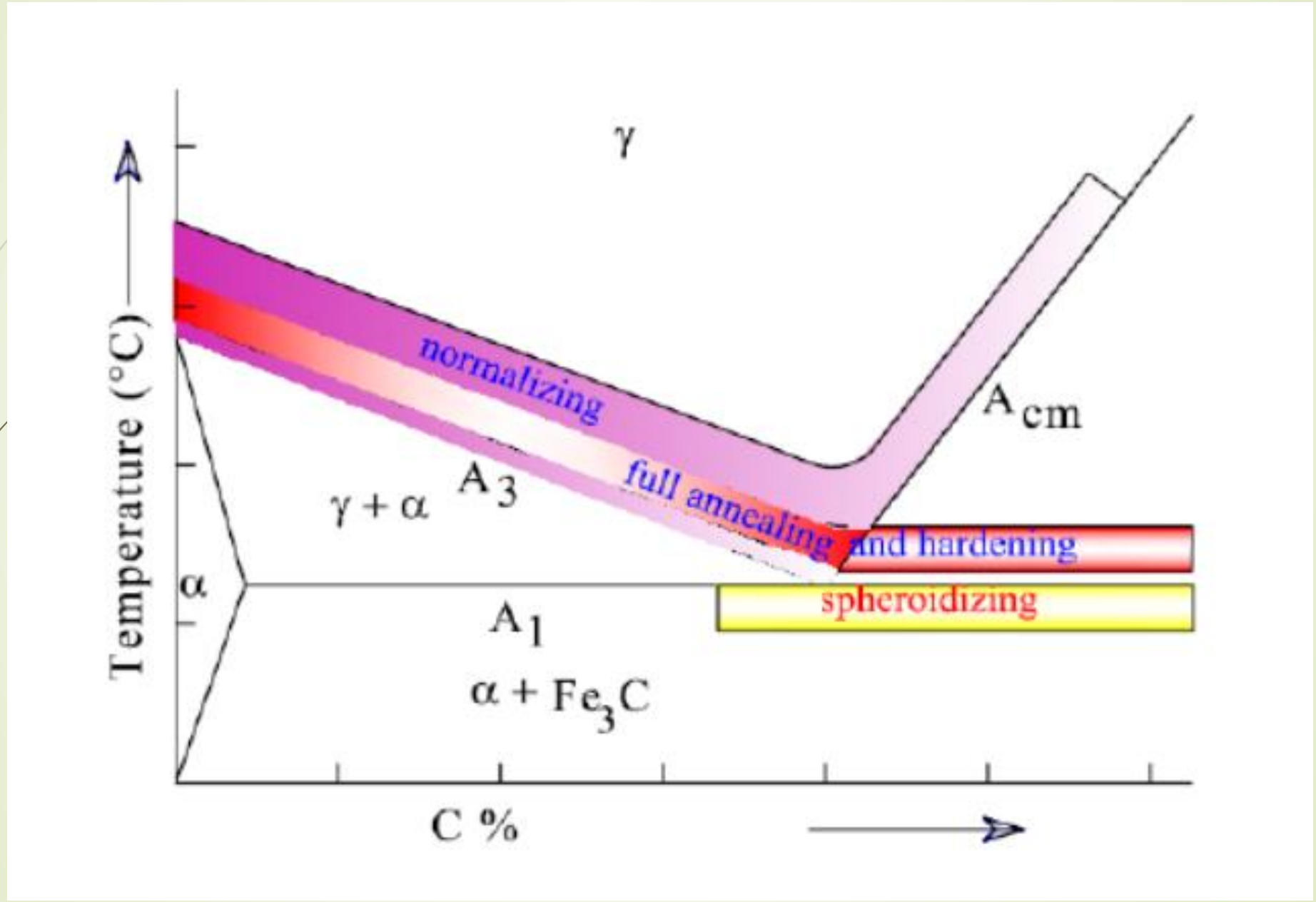
γ
normalizing
full annealing
A cm
γ + α
A 3
and hardening
spheroidizing
α
A 1
α + Fe3C
Temperature (°C)
C %

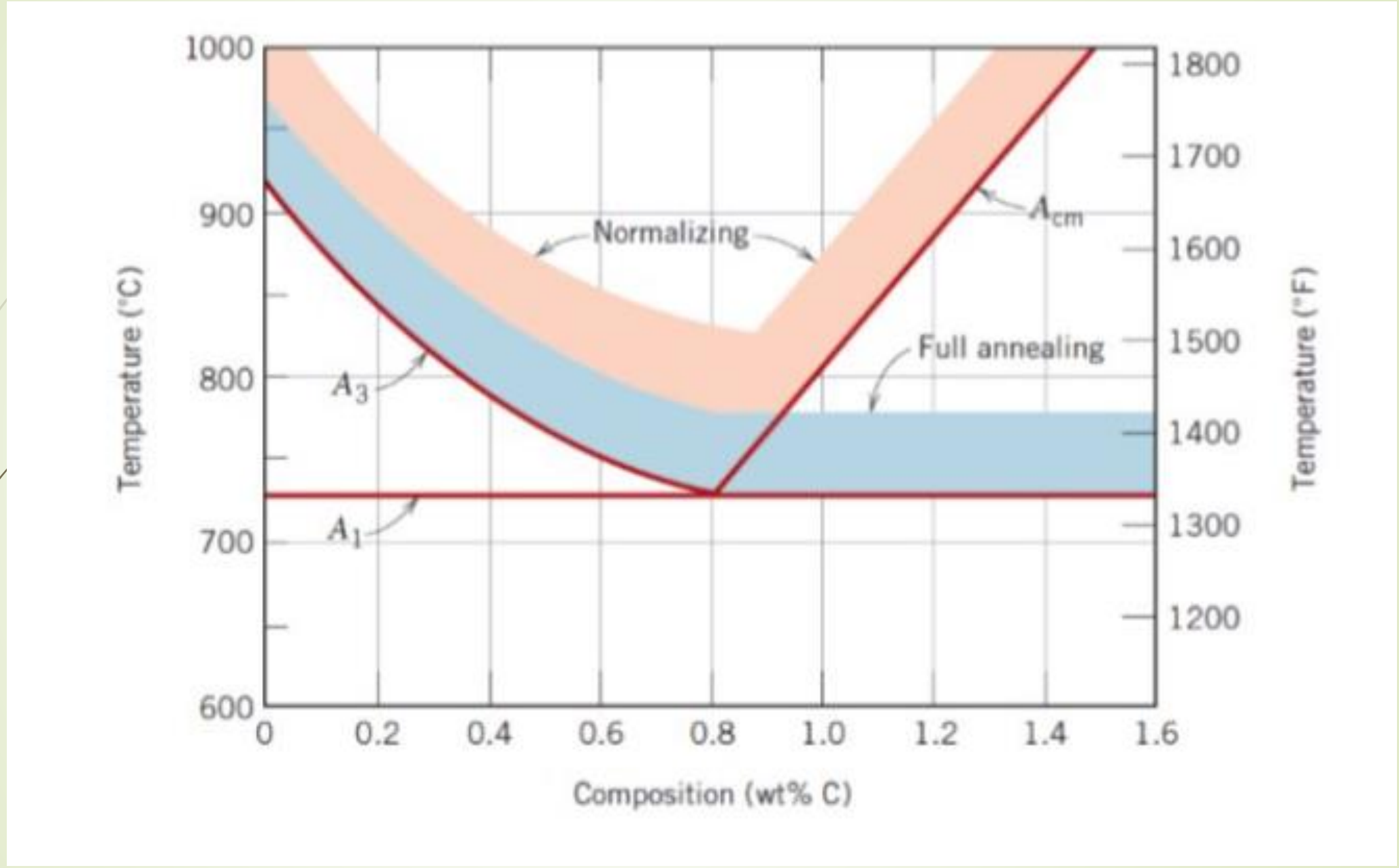
1000
900
800
700
600
1800
1700
1600
1500
1400
1300
1200
0
0.2
0.4
0.6
0.8
1.0
1.2
1.4
1.6
Temperature (°C)
Temperature (°F)
Composition (wt% C)
Normalizing
Full annealing
A_3
A_1
A_{cm}

عملیات حرارتی استمپرینگ وکوانچ وتمپر

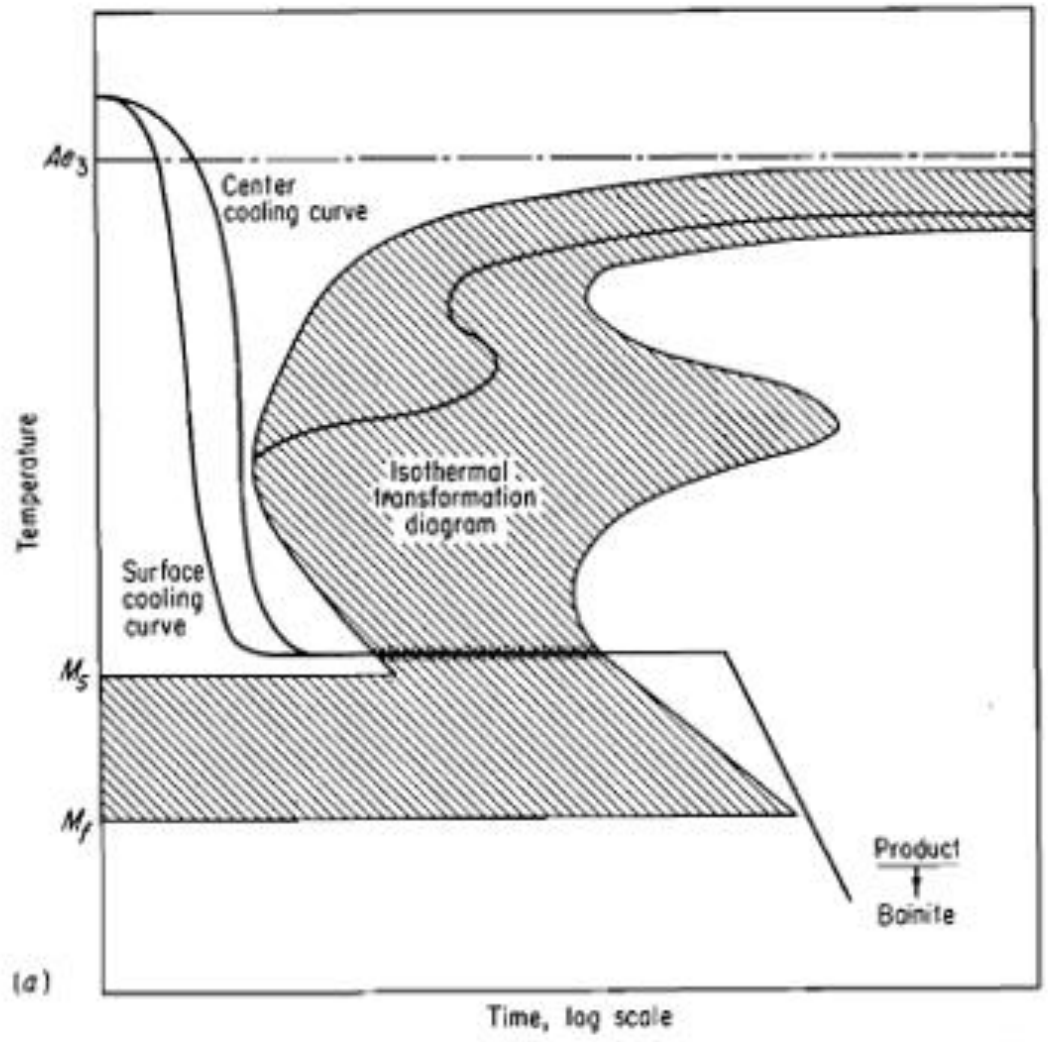

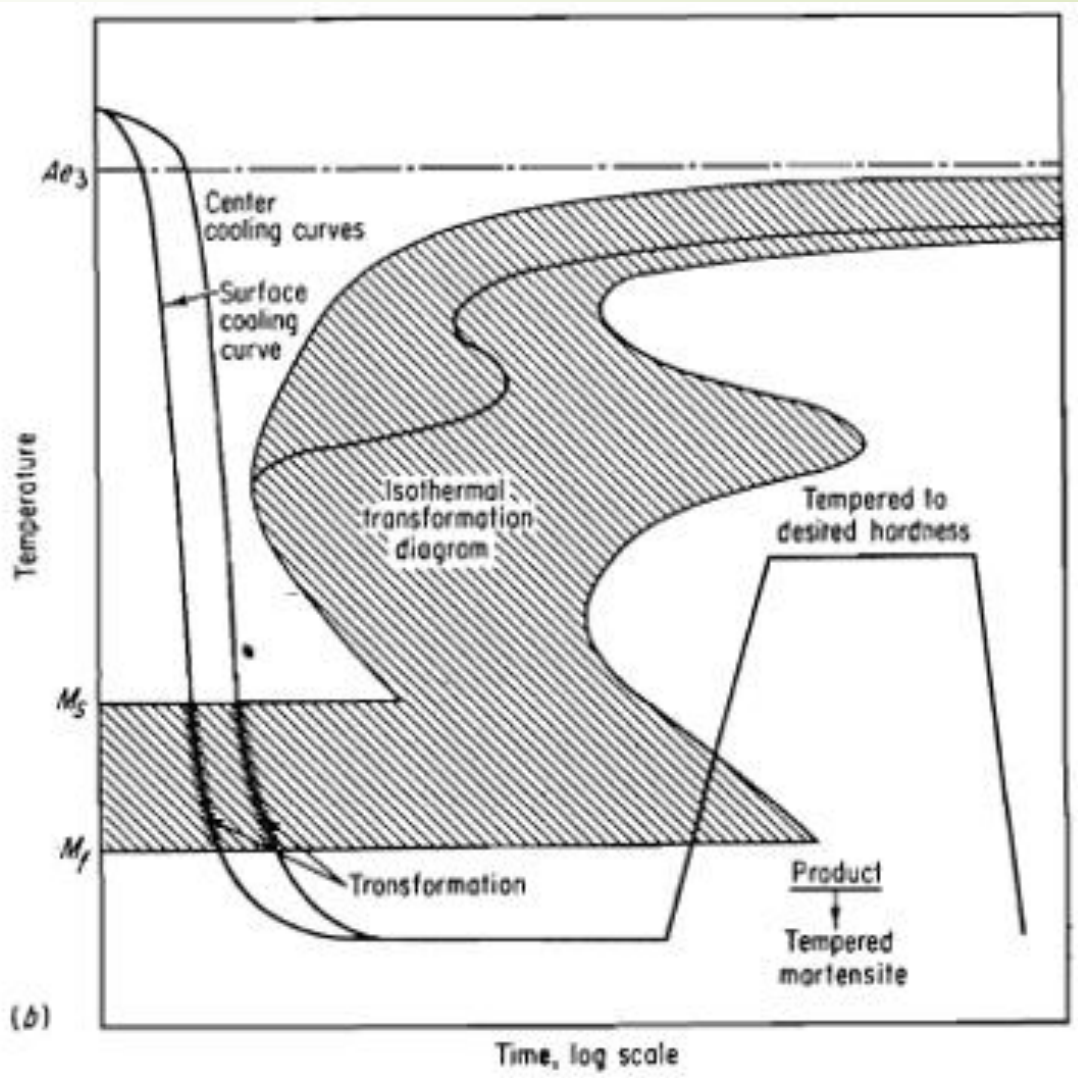

عملیات حرارتی مارتمپرینگ یا مار کوانچینگ

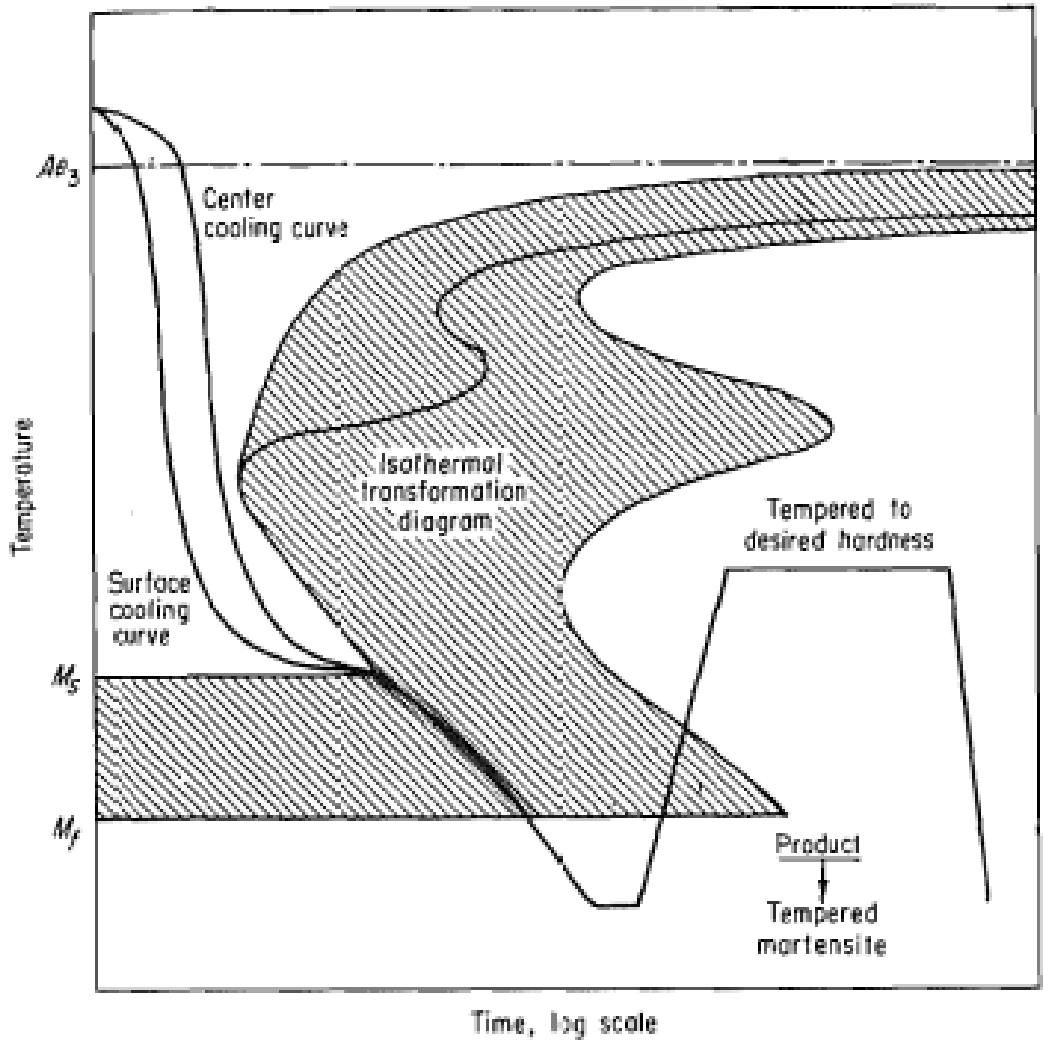

Fig. 8-86 Schematic transformation diagram illustrating martempering or marquenching. (From "U.S.S. Carilloy Steels," U.S. Steel Corporation.)

انواع مختلف فرایند های کوانچ

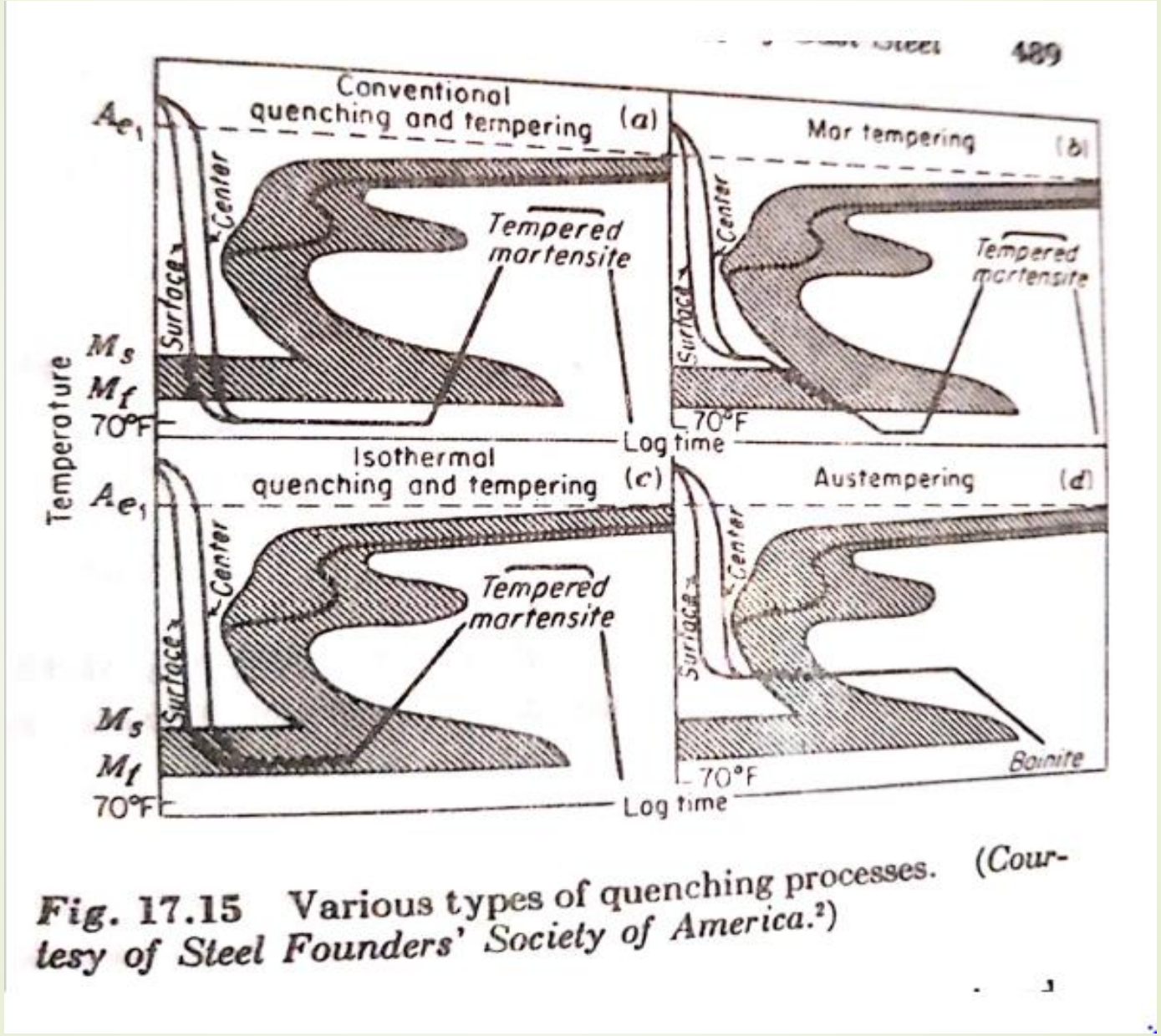

Fig. 17.15 Various types of quenching processes. (Courtesy of Steel Founders' Society of America.[2])

منحنی های سرد کردن

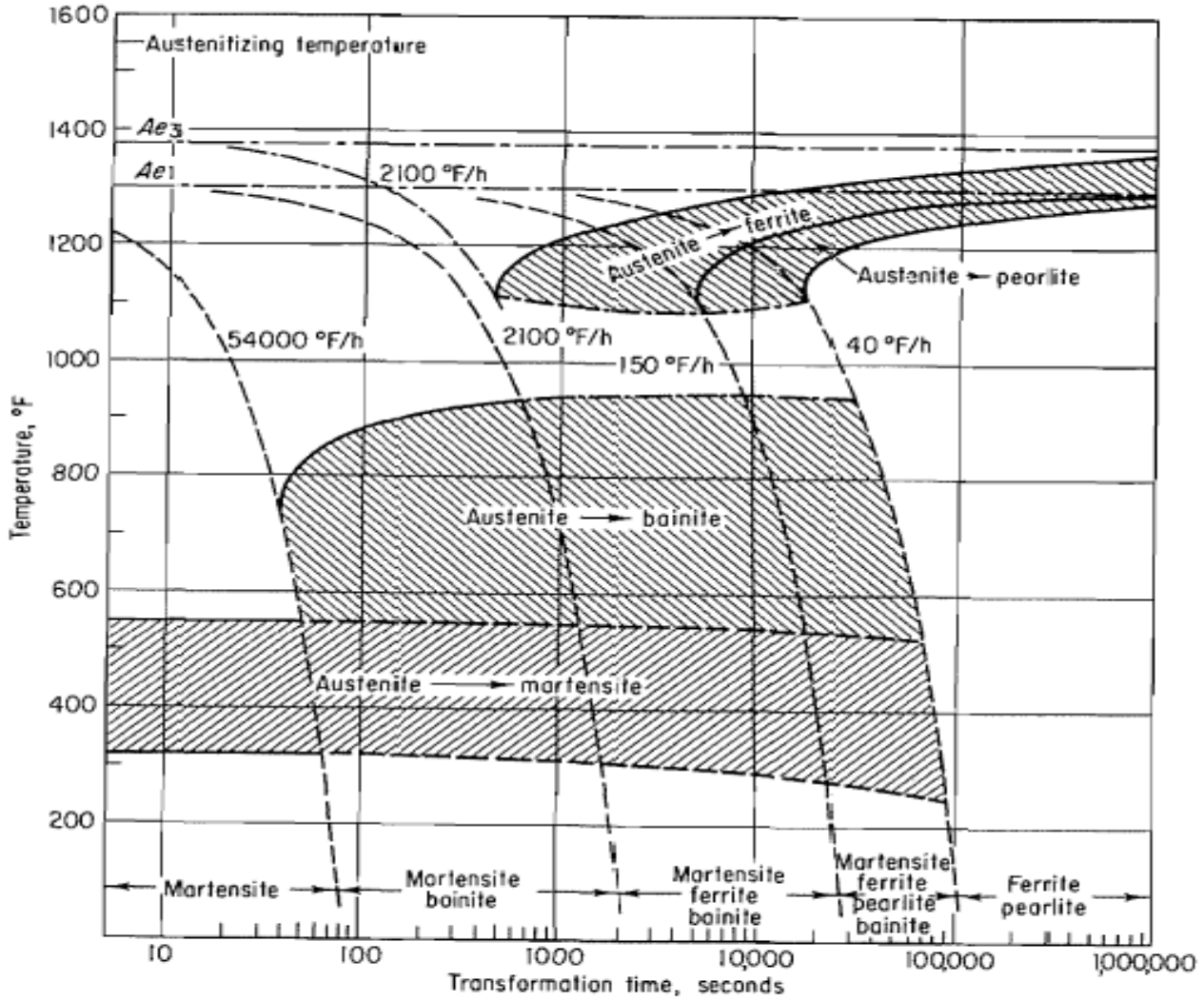

Fig. 8-26 C-T diagram of a triple-alloy steel (4340): 0.42 percent carbon, 0.78 percent manganese, 1.79 percent nickel, 0.80 percent chromium, 0.33 percent molybdenum. (From "U.S.S. Carilloy Steels," U.S. Steel Corporation.)

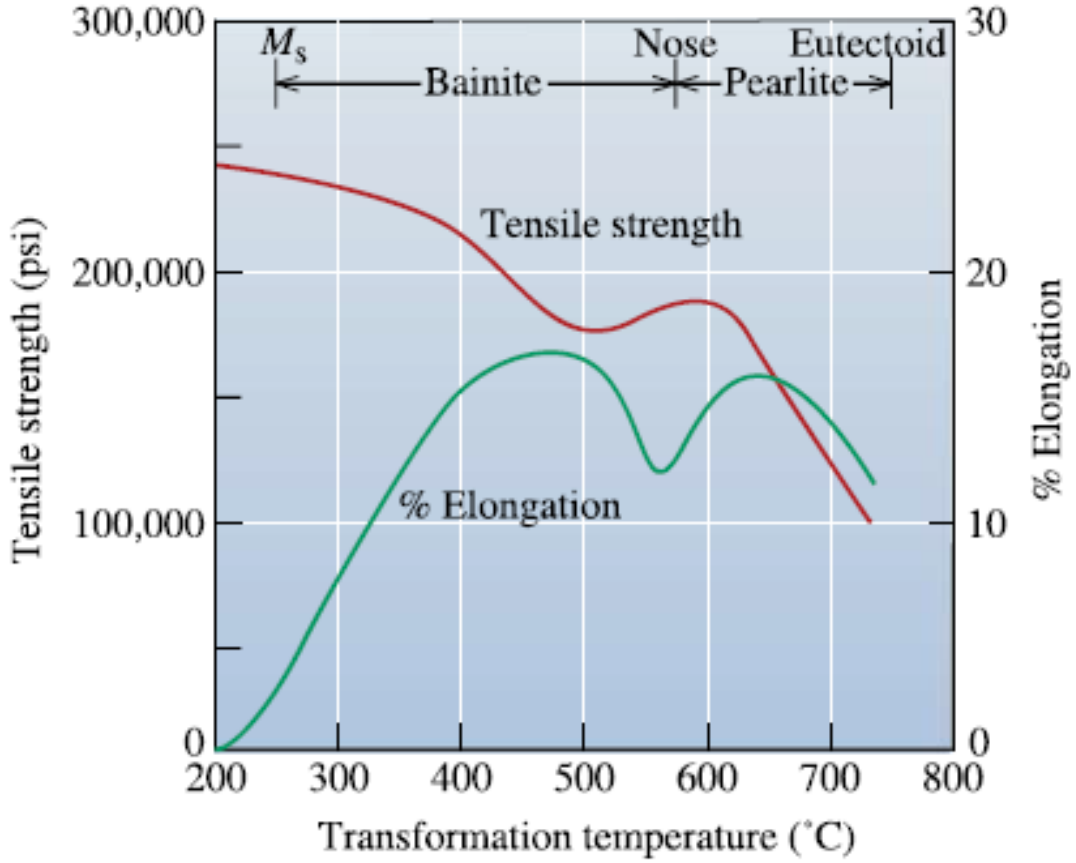

Figure 12-23
The effect of transformation temperature on the properties of a eutectoid steel.

دیاگرام یوتکتیک

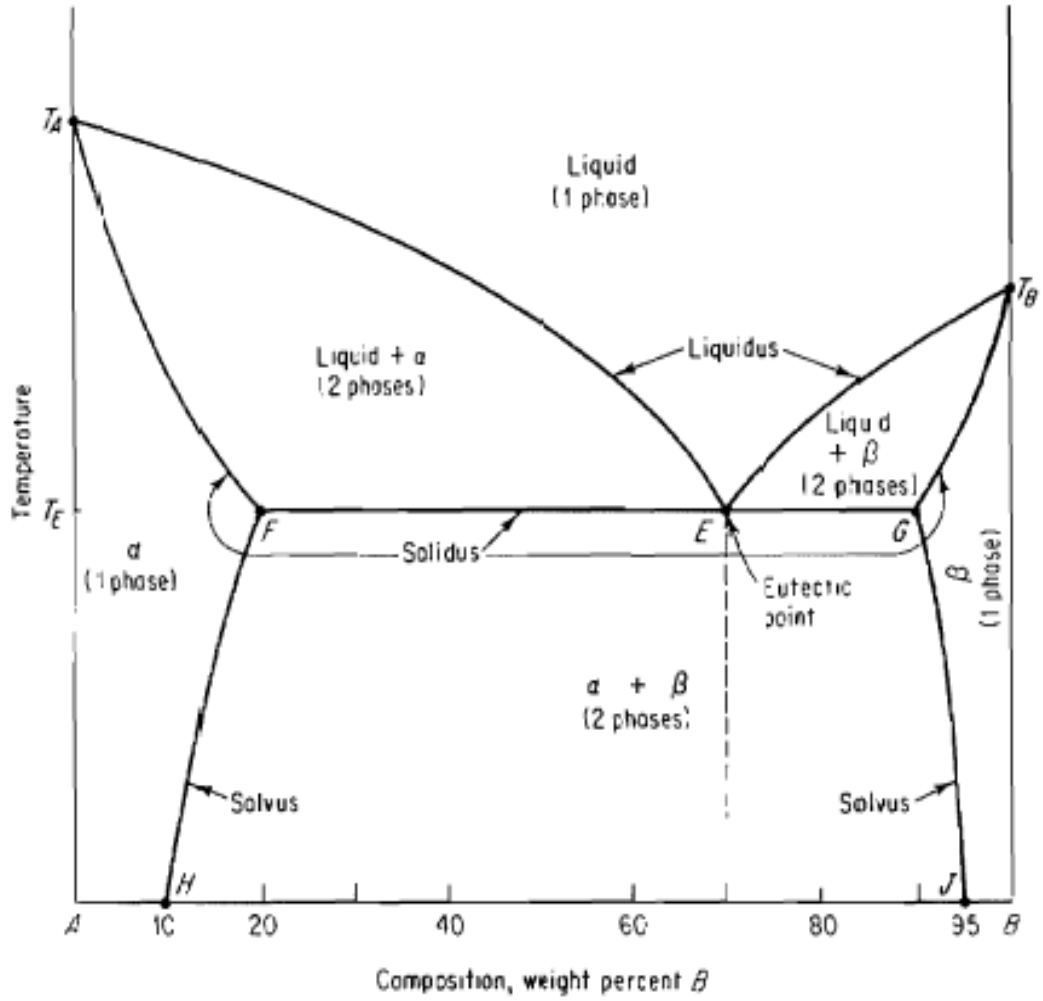

Fig. 6-23 Phase diagram illustrating partial solid solubility.

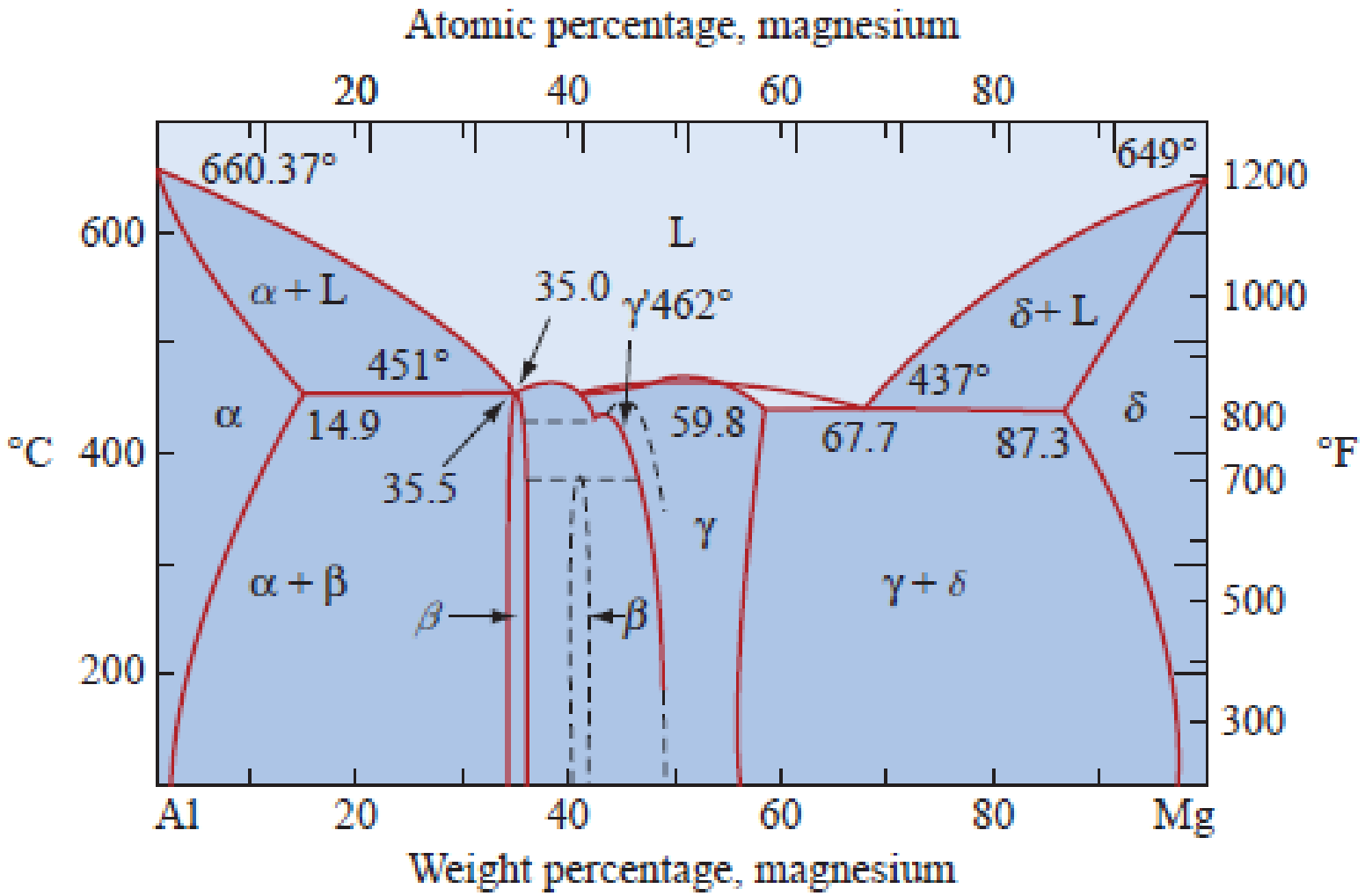

Figure 12-10 The aluminum-magnesium phase diagram.